THEORY

PIPEBREAK MODEL

DATE: December 2023

The model PIPEBREAK models the two-phase discharge from a long pipeline. This report documents the theory underlying the model and includes also validation results.

Reference to part of this report which may lead to misinterpretation is not permissible.

No.	Date	Reason for Issue	Prepared by	Verified by	Approved by
1	Aug 2001	PHAST 6.1	Webber & Witlox	Witlox	
2	Oct 2005	SAFETI 6.5	Harper		
3	April 2010	Phast 6.6	Stene		
4	April 2011	Phast 6.7	Stene		
5	May 2021	Apply new template	D. Vatier		
6	July 2022	Update for Phast 8.7	A. Oke		

Date: December 2023

Prepared by: Digital Solutions at DNV

© DNV AS. All rights reserved

This publication or parts thereof may not be reproduced or transmitted in any form or by any means, including copying or recording, without the prior written consent of DNV AS.

ABSTRACT

Pressure-liquefied gases are routinely transported along pipelines many kilometres in length. The possibility of an accidental breach of such a pipeline forms a potentially severe hazard, which may lead to a large dispersion source term or more directly to a fire or explosion.

Models of flows in long pipelines exist which are complicated (relying on a full CFD solution of time-dependent Reynolds equations), or applicable only to gases, or applicable (explicitly or implicitly) only to simple thermodynamics and relatively small pressure drops.

One of the substances of interest is ethylene, with a critical temperature around 10 Celsius, and which may be pumped along pipes at pressures approaching 100 Bar. We have therefore derived a mathematical two-phase flow model called PIPEBREAK, which admits an appropriate thermodynamic description and is formulated in such a way that no thermodynamic singularities appear at the critical point. Furthermore it is constructed without recourse to any simplifying assumptions which might become less accurate at large pressure drops, and covers both choked and unchoked flow conditions. It therefore applies to any fluid which boils significantly below ambient temperature. Nevertheless it is a simple, explicit, and transparent integral model involving clear physical assumptions. It leads to predictions of the evolution of the pressure and temperature at the outlet and at the upstream end of the pipe and of the mass flow rate out of the breach, which depend on no free parameters. Computationally it requires only knowledge of a few thermodynamic properties of the substance involved, and the ability to do explicit definite integrals - for example by Simpson's rule.

We show that the model fits experimental data on propane releases from a 100m pipe breached suddenly at one end (the Shell "Isle of Grain" trials) at least as well as more complicated models. The PIPEBREAK model is a new model including all relevant physics, but which is simple and requires little CPU time. It can be used routinely by engineers for practical situations.

This document presents the theory behind the model PIPEBREAK. It is designed specifically to be a complete and self-contained explanation of the model for a full-bore rupture at the end of the pipe. It also adds detail on smaller breaches and introduces breaches at other points on the pipe, and the effects of valve closure.

Table of contents

Table of Figures[1]

[1] **Spreadsheet for Figure 12,** Figure **13** and Figure 14: Pbrk_Validation_IsleOfGrain.xls

1 INTRODUCTION

This document describes the theory on which the code PIPEBREAK is based. Much of the main development of the model has been presented by Webber, Fanneløp, and Witlox (1999)[1] in a paper published in the proceedings of the 1999 CCPS Conference in San Francisco, and this document follows that paper - as it was designed specifically to be a complete and self-contained explanation of the model for a full-bore rupture at the end of the pipe. This document also adds more detail on smaller breaches and introduces breaches at other points on the pipe, and the effects of valve closure.

Scope

PIPEBREAK is model of two-phase flow in a pipe of uniform cross-section following an accidental breach. Two-phase flow will be important in any breach of containment of gases which are stored or transported as pressurised liquids. A specific objective is a model which will comprehend the behaviour of ethylene, which may be pumped at pressures approaching 100 Bar and which has a critical temperature around 10 Celsius. It is therefore important that our model should not break down at large pressure differences or in the vicinity of the critical point or for very long (many km) pipelines.

It is also important that the model should comprehend the behaviour of propane at much more modest pressures, with a critical point further removed from the thermodynamic region of interest, and in shorter (100m) pipes as the Shell Isle of Grain experiments on propane (Cowley and Tam, 1988)[2] constitute a very useful data set for model validation. These data have recently been summarised by Richardson and Saville (1996)[3] who also compare their model with the data and set a standard for the kind of agreement which is possible. However, from their qualitative description, their model is apparently rather complex and they place great weight on an accurate understanding of the thermodynamics of multi-component hydrocarbons. We shall derive a simpler model, and in our concluding sections we shall discuss it with reference to the Isle of Grain data, and in comparison with the single-phase gas flow model of Fanneløp and Ryhming (1982)[4] and the two-phase flow models of Leung and co-workers [e.g. Leung (1986)[5]] and of Richardson and Saville (1996)[3].

Organisation

The base case for consideration will be a full bore rupture at the end of a pipe. This case will be developed in full detail in what follows. Other cases, including a smaller rupture at the end of the pipe and a breach at an arbitrary point in the pipe will then be described in terms of the base case. The model will also be extended to allow for closure of valves during an accident.

2 A PIPE WITH A FULL BORE RUPTURE AT ONE END

This part of the manual gives a detailed derivation of the model for a pipe of uniform cross-section with a full bore rupture at one end.

2.1 The model

The model postulates that following a breach in the pipeline there will in general be four successive flow regimes.

Regime i - rapid depressurisation.
Immediately following the breach, the pressure in the pipe will decrease from the operating pressure very rapidly. The rate of drop will be governed by the speed of sound in the liquid (or supercritical fluid) in the pipe and we assume that this process ends with the fluid as saturated liquid at some temperature T_0 and pressure $p_0=p_{sat}(T_0)$. Thermodynamically this process may be complicated by shock waves in the pipe, and there is some uncertainty in the degree of cooling expected. Dynamically it may be slightly affected by the non-rigidity of the pipe itself (elasticity of the pipe wall). However, we expect any expansion, and hence ejection of fluid from the breach, to be governed primarily by the compressibility of the liquid, which is small, especially on the scale of later expansion due to vaporisation. Our estimates of this regime therefore result in the conclusion that this process happens very quickly compared with what follows, and that the loss of fluid is small, also compared with what follows.

We shall also assume that during this regime the fluid comes effectively to rest (if any pumped inflow is cut off by valve closure) or to a flow rate governed by the pump (if it is not). In fact this process is likely to be rather violent and one must question the survivability of any pumps and valve mechanisms, but that depends on their design and is outside the scope of this work.

Estimating the temperature T_0 achieved during this regime may involve some uncertainty as it is unlikely to be as simple as isentropic, isenthalpic, or isothermal expansion. However, for the current purposes, we shall simply note that in the Isle of Grain trials the propane pressure appears to have dropped very rapidly with no significant temperature decrease - but we also observe for future reference that the pressure drop from about 11bar to the saturated vapour pressure of around 8bar is relatively modest compared with what may be expected in some situations of interest.

Regime ii - flash front propagation or erosion of the saturated liquid zone
Following regime i, we have a pipe containing saturated liquid at rest or being pumped at some given flow rate. It will start to vaporise and depressurise further, extracting heat from the fluid itself and the surrounding pipe wall. We expect vaporisation to start at the breach where the fluid sees the ambient pressure environment and, considering for the moment a pipe closed at its upstream end, our model for this regime is one of two fluid zones as shown in Figure 1.

The upstream zone (Zone 1) is saturated liquid at rest at constant temperature T_0 and pressure $p_0=p_{sat}(T_0)$. Fluid is flowing from the interface (b) to the breach (e) and as it moves downstream, the gas fraction increases and the pressure decreases to some value p_e at (e). The flow rate through Zone 2 is coupled with the pressure drop and the rate of expansion due to vaporisation between (b) and (e). As the mass of fluid in the pipe decreases, the Zone interface (b) moves upstream, and forming a flash front which erodes the liquid zone 1.

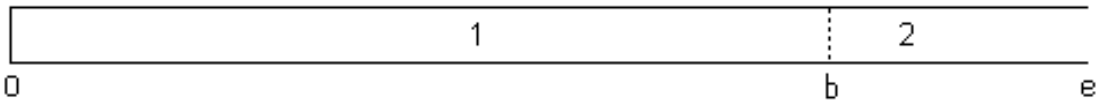

Figure 1. Flow in regime ii (flash-front propagation) in a pipe closed at the upstream end
Zone 1 is saturated liquid at rest. Zone 2 is two-phase fluid flowing from left to right and out of the breach (e). The gas fraction in Zone 2 increases from zero at the zone interface (b) as one goes downstream to the breach (e).

Initially at least, the flow is expected to be choked at (e) and the exit pressure p_e will be greater than the ambient pressure p_a. At the onset of regime ii the saturated liquid is assumed to fill the pipe. That is to say that the flash front (b) initially coincides with the exit (e) and the exit pressure p_e starts at p_0. In order to achieve this consistently, the initial flow rate out of the exit must be that which corresponds with a choke pressure equal to p_0, and, as we shall see, this criterion alone gives a remarkably accurate prediction of the initial rate of mass loss.

Ultimately the flash front (b) will encounter the closed upstream end of the pipe, and this signals the end of regime ii and the onset of regime iii.

If, instead of a closed upstream end, we have a constant inflow, then the flash front may ultimately be arrested at some point in the pipe when the outflow at the breach balances the inflow. In this case a steady flow will be set up and regime iii will not be relevant.

Regime iii - continuing, two phase flow.
After the flash front encounters the closed upstream end of the pipe, then the two-phase zone, Zone 2, will fill the pipe. Only at this point will the upstream pressure start to drop. It will continue to drop until both the upstream and exit pressures reach the ambient value and there is no thermodynamically induced pressure gradient to drive flow out of the pipe.

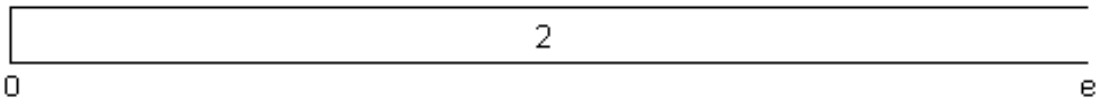

Figure 2. Flow in regime iii (continuing two-phase flow) in a pipe closed at the upstream end
The flash front has reached the upstream, closed end of the pipe and the two-phase zone, Zone 2, now fills the entire pipe. There is still a significant gradient of pressure and liquid fraction along the pipe, and vaporisation is still driving fluid out of the breach.

Regime iv - unpressurised flow.
At the end of regime iii, almost all the mass of fluid will have been forced out of the pipe. The liquid component of any small amount remaining will be expected to settle in the pipe and any further flow will be governed by slow evaporation from the now cold pipe and gravity flow. The mass release rate will be very small compared with that in regimes ii and iii and we shall neglect it here.

Thus we see, from the point of view of hazard analysis, that regimes ii and iii are the most important ones to consider in detail and this is where our detailed modelling below will apply.

Before going on to define the model quantitatively, one or two comments are in order. Firstly we have also considered the possibility that there may be a third zone in the pipe, downstream of Zone 2, in which all the liquid has vaporised and we have pure gas flow. However, the heat available from the liquid itself is usually insufficient to achieve this in fluids of interest and our estimates of possible heat transfer rates from the pipe wall also lead us to believe that the fluid will remain in a two-phase state for the entire time under consideration. Secondly, the assumption of the above flow regimes is we believe very plausible, and is what renders the calculations below so tractable. Further assumptions below are very much within this framework. The framework itself can be tested in principle, for example by applying a large Computational Fluid Dynamic code to the problem, which makes no such assumptions, and examining the results to see to what extent the regimes ii and iii can be identified. However, we believe there is some fairly direct evidence for these regimes from the Isle of Grain experiments, as we shall discuss below.

Finally we should emphasise that we are explicitly considering approximately horizontal pipelines. However in regimes ii and iii where the mass release rates are greatest, the mass is effectively pushed out by the thermodynamic forces vaporising the liquid. These can be expected to dominate the gravitational forces as long as the gravity head is not too large. Gravity effects may be very important in regime iv, but the mass released in that regime will be small for the two-phase flows we are considering. Therefore we shall neglect gravity. (The importance of gravity can be estimated post-hoc simply by comparing the predicted pressure differences with the gravity head.)

2.2 Homogeneous Equilibrium Thermodynamics

Experimental evidence
Before looking at the fluid dynamic aspects of the problem in more detail, we know we are going to need to make assumptions about the thermodynamic nature of the two-phase flow. A popular, and attractively simple, assumption is that the phases remain in thermodynamic equilibrium. But this assumption is so crucial to the flow dynamics that it would be reassuring to have some experimental evidence that this may be the case. Happily there is some very good evidence. The Isle of Grain propane experiments presented measurements of the temperature and pressure at the ends of the pipe and how they varied together in time. It is a simple matter to plot the measurements of pressure against temperature and superimpose these on the known vapour pressure curve of propane [Reid, Prausnitz and Poling (1987)[6]].

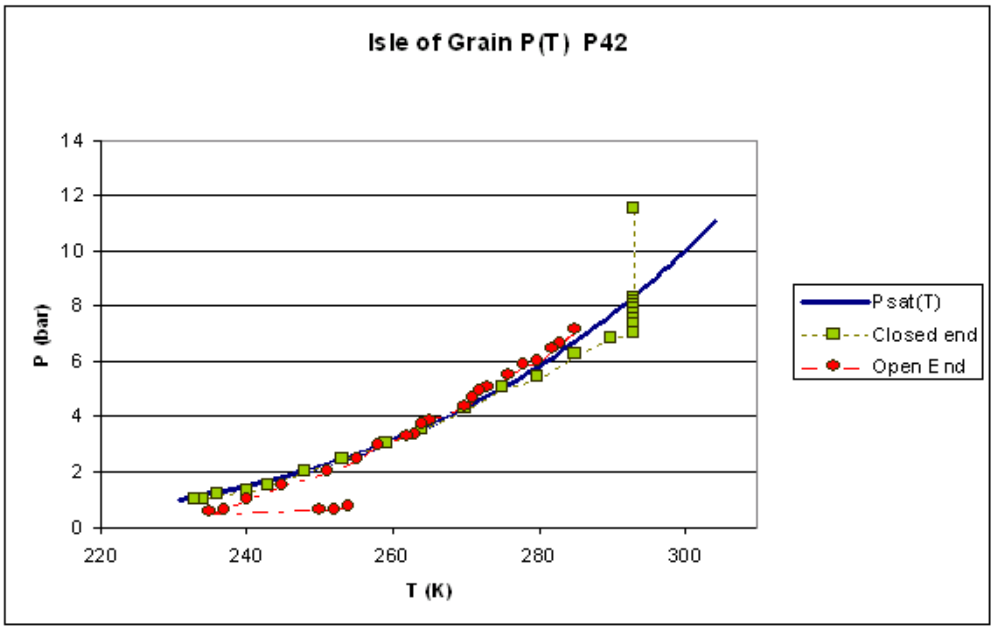

Figure 3. **Pressure and temperature for Isle of Grain Trial P42**
The measured values at the closed and open ends are superimposed on the saturated vapour pressure curve p = $p_{sat}(T)$ of propane.

We show the results for trial P42 in Figure 3, in which the line represents the vapour pressure curve of propane, and the square and diamond points represent the experimental measurements at the upstream (closed) and downstream (open) ends respectively. The time evolution in the experiments, from top right to bottom left, is indicated by the broken lines.

The results of this plot are very revealing. First the p(T) relationship at both ends is spectacularly close to the vapour pressure curve and we need have no further doubts about using the homogeneous equilibrium model, at least for the propane pipeline used in these experiments.

There are two areas where the experimental values depart from the curve. At the top right, the first point at the closed end represents the initial pressure which was well above the saturated vapour pressure at the (ambient) initial temperature. The immediate and apparently isothermal (in this case) pressure drop to the vapour pressure curve is exactly what we have described in regime i above. From then on the results adhere to the vapour pressure curve until at the open end there is ultimately an increase in temperature at constant ambient pressure. Examination of the mass inventory at this point shows that essentially all of the mass has been expelled from the pipe by this time, and that we are seeing a warming after the experiment is effectively over and the liquid has vaporised - regime iv above.

We regard this as very strong support for the homogeneous equilibrium model (in the two-phase flow Zone) which we shall adopt below. It is also entirely consistent with the flow regimes assumed above.

Equations of state

Adopting the homogeneous equilibrium model for all two-phase flow zones of regimes ii and iii allows us to relate temperature and pressure everywhere by

$$T = T_{sat}(p) \qquad or \qquad p = p_{sat}(T) \tag{1}$$

The specific volume v and specific enthalpy h can both be expressed in terms of the local liquid mass fraction η as

$$v = \eta v_L + (1-\eta)v_v \tag{2}$$

$$h = \eta h_L + (1-\eta)h_v \tag{3}$$

where subscripts L and v refer to the liquid and vapour components. In fact we shall not need the mass fraction explicitly in our calculations, and eliminating it gives

$$h = h_L + (v - v_L).\phi \qquad (4)$$

where

$$\phi(T) \equiv \frac{h_v - h_L}{v_v - v_L} = T\frac{dp}{dT} \qquad (5)$$

The last equality (the Clapeyron Equation) is an exact, general thermodynamic property, and it means that the thermodynamic properties needed for this model will almost entirely be restricted to the vapour pressure curve $p=p_{sat}(T)$, the liquid specific volume at saturation $v_L(T)$, the liquid specific enthalpy $h_L(T)$ at saturation. These are assumed known, and in particular ϕ is a thermodynamic property (with the dimensions of pressure and which is defined along the vapour pressure curve) which will appear throughout our model as it defines the homogeneous equilibrium model's two-phase equation of state for h(T,v).

2.3 One-dimensional flow

The model

Our starting point is a one-dimensional flow model, which may be described by the mass, momentum, and energy equations. Denoting t=time and x=downstream distance, we have

$$\frac{\partial}{\partial t}\left(\frac{1}{v}\right) + \frac{\partial G}{\partial x} = 0 \qquad (6)$$

$$\frac{\partial G}{\partial t} + \frac{\partial (G^2 v + p)}{\partial x} = -2f\frac{G|G|v}{D} \qquad (7)$$

$$\frac{\partial([h + pv + G^2v^2/2]/v)}{\partial t} + \frac{\partial([h + G^2v^2/2]G)}{\partial x} = \frac{4q}{D} \qquad (8)$$

in which we have focused on the mass flux density G [dimensions $ML^{-2}t^{-1}$], the fluid specific volume v [L^3M^{-1}], pressure p [$ML^{-1}t^{-2}$] and the fluid specific enthalpy h [$EM^{-1} = L^2t^{-2}$]. The other quantities are the pipe diameter D [L], the Fanning friction coefficient f [dimensionless], and the heat flux density q(x) [$EL^{-2}t^{-1} = Mt^{-3}$] from the pipe wall into the fluid. In what follows we shall use subscript '0' to refer to upstream conditions and subscript 'e' to refer to conditions at the exit.

It is convenient to eliminate the related fluid density $\rho=1/v$ and velocity $w=Gv$ in favour of the above variables. The total mass flow rate from the breach is GA where $A=\pi D^2/4$ but again it is convenient to work almost exclusively in terms of quantities per unit cross-sectional area of pipe.

These equations together with the equations of state (1), (4) form a closed set for the five quantities p,v,G,T,h, as long as we know the heat transfer rate q. We shall seek separate approximations within the context of regimes ii and iii above to render them more analytically tractable.

The mass integral

Before going on to look separately at the details of regimes ii and iii, let us note some of the common points of the methods which will be used. We can integrate the mass equation (6) along the whole length of the pipe to obtain the rate of change of the total mass of fluid (per unit area) in the pipe:

$$\frac{dM}{dt} = G_0 - G_e \qquad (9)$$

where G_0 is the in-flow at the upstream end and G_e is the outflow at the breach. $G_0(t)$ will be prescribed as zero for a closed pipe or to be some rate determined by pumping. G_e remains to be predicted but will decrease monotonically in

time through regimes ii and iii, and it can therefore be used as a measure of time. Similarly the pressure decreases monotonically along the pipe and at any given time can be used for much of the calculation as a measure of distance.

Our method will use the momentum and energy equations to predict the upstream and downstream pressures $p_0(G_e^2)$, $p_e(G_e^2)$ as functions of this release rate, the specific volume of the fluid along the pipe as $v(p,G_e^2)$, and ultimately the mass $M(G_e^2)$. Pressure will be related to distance by an equation involving dp/dx, and mass to time by (9). The last step of the method will compute the time at which a particular value of G_e is achieved by integrating (9) in the form

$$t = \int_{M}^{M_{init}} \frac{dM}{(G_e - G_0)} \qquad (10)$$

where subscript "init" refers to the initial value at time t=0. Some care is required with the singularity when G_0 is non-zero, but at least the singularity is explicit and appropriate mathematical techniques can be adopted to handle it. This integral can be performed through regimes ii and iii after all separate considerations have been taken into account in obtaining $M(G_e^2)$.

2.4 Flow in Regime ii - Modelling the Flash Front

The flow model in regime ii

The essential features of this regime ii are the initially choked exit pressure and the flash front moving into the saturated liquid zone.

We expect the flash front to be moving slowly compared with the fluid velocity out of the exit and it is therefore appropriate to consider the flow in the two-phase zone in this regime as quasi-steady. Considering for the moment the case q=0 of zero heat transfer from outside the fluid, the mass, momentum and energy equations in the steady flow limit (obtained by setting the $\partial/\partial t$ terms above to zero) tell us that G is uniform along the flow in the two-phase zone, that

$$\frac{d(G^2 v + p)}{dx} = -2f\frac{G|G|v}{D} \qquad (11)$$

and that

$$h + G^2 v^2/2 = E \qquad (12)$$

is also uniform along the flow. These equations are used to describe Zone 2 in Figure 1 while the saturated liquid in Zone 1 remains at rest uniformly and constantly at (p_0,T_0). Here E is a constant of integration - the "stagnation enthalpy" - ie the enthalpy at a (usually fictitious) point where the velocity w=Gv is zero.

Heat transfer from the pipe wall

We have explored various ways of allowing for heat transfer from the pipe wall. Our conclusions are that heat from the steel pipe itself is relatively readily available to aid vaporisation, but that heat from outside the pipe is much less readily available. We can idealise this situation in the case of quasi-steady flow by demanding that the local temperature in the steel wall closely matches the neighbouring fluid temperature at all times. Thus we give the fluid immediate access to any heat stored within the pipe wall.

Implementing this approximation in the model results in a modification to the energy equation to give

$$h' + G^2 v^2/2 = E \qquad (13)$$

where h' is an effective specific enthalpy given by

$$h'(v,T) = h(v,T) + \frac{\rho_s}{\rho_L}\frac{4Y}{D}c_s T \qquad (14)$$

in which ρ_S, c_S, Y are the density, specific heat, and thickness of the steel pipe wall. In what follows we'll drop the primes and write simply "h" with the understanding that if heat transfer is to be included in regime ii, then the last term of (14) must be included in the definition.

Boundary conditions - choked and unchoked flow

The upstream boundary conditions, applied to Zone 2 in Figure 1, give values T_0, $p=p_{sat}(T_0)$, $v_L(T_0)$, $h_L(T_0)$ at the flash front (b) in Figure 1. The as yet unknown mass flux density G is supplied by a down-stream boundary condition:

$$p_e = \max(p_a, p_{choke}(G)) \qquad (15)$$

which we shall now explore.

Choked flow in the simple, steady, one-dimensional flow model presented above is most clearly understood by writing the steady momentum equation in the form:

$$\left[G^2 \frac{dv}{dp} + 1 \right] \frac{dp}{dx} = -2f \frac{G|G|v}{D} \qquad (16)$$

For any given G, sooner or later (in general) there will occur a point in the flow where dv/dp reaches a value of $-1/G^2$. At this point the fluid has reached its local speed of sound and dp/dx will be negative and infinite (although p will be finite). We cannot advance beyond this point in x and if this happens in the pipe, it can only be at the exit. Thus the choke equation

$$\frac{dv}{dp} = -\frac{1}{G^2} \qquad (17)$$

yields a choke pressure $p_{choke}(G)$ which gives the downstream boundary condition (15). In order to evaluate the choke pressure we first need the function v(p).

The steady solution

The energy equation (12),(13) and the equation of state for enthalpy (4) may be combined to eliminate h yielding:

$$v = \frac{1}{G^2}\left[-\phi + \sqrt{\phi^2 + 2G^2(E + v_L\phi - h_L)} \right] \qquad (18)$$

Knowledge of how the thermodynamic functions ϕ, v_L, and h_L depend on T, and hence through the saturation curve on p, makes this a prediction of the variation v(p) along the pipe. It is well defined at small mass flow rates with the limit

$$v \xrightarrow[G\to 0]{} \frac{E + v_L\phi - h_L}{\phi} \qquad (19)$$

The assumption or derivation of a profile v(p) along the pipe is crucial to all analytic solutions of pipe flow problems and we shall discuss the relationship of this one with those of Fannelop and Ryhming (1982)[4] and of Leung and collaborators - eg Leung (1986)[5] - below.

With the profile v(p) we can use the momentum equation to derive the variation p(x) of pressure along the pipe implicitly in the inverse form x(p)

$$x(p) = \frac{D}{2f}\left[\frac{1}{G^2}\int_{p_e}^{p} \frac{dp}{v} - \ln\left(\frac{v_e}{v}\right) \right] \qquad (20)$$

where in this equation it has proved convenient to change to measuring distance x upstream from the exit point to the point where the pressure and volume are (p,v). In general the integral can be done numerically very quickly. We can thus, given the mass flux density G, determine the profile of all relevant quantities along the pipe through the two-phase zone. In particular the length L_2 of the two-phase zone can be found for given G^2, by integrating up to p_0.

The choke pressure and the initial flow rate

As we have already seen, we also need the pressure derivative dv/dp, and with a little algebra this turns out to be

$$\frac{dv}{dp} = -\frac{1}{(G^2 v + \phi)}\left[(v - v_L)\frac{d\phi}{dp} + \frac{dh_L}{dp} - \phi\frac{dv_L}{dp} \right] \quad (21)$$

where of course all pressure derivatives on the right hand side may be written as temperature derivatives using

$$\frac{d}{dp} \equiv \frac{dT}{dp}\frac{d}{dT} \equiv \frac{T}{\phi}\frac{d}{dT} \quad (22)$$

Fluid dynamically they are just total derivatives along the flow; thermodynamically they are partial derivatives along the saturation curve, and are assumed known for whatever substance is being considered.

The choke condition (17) therefore relates the choke pressure implicitly to G through

$$\left[(v - v_L)\frac{d\phi}{dp} + \frac{dh_L}{dp} - \phi\frac{dv_L}{dp} - v \right] G^2 = \phi \quad (23)$$

This can be solved for known thermodynamic properties and using $v(p,G^2)$ as given above to give $p_{choke}(G^2)$ or $G^2(p_{choke})$. A special case is the initial flow rate which corresponds with a choke pressure equal to the initial pressure $p_0=p_{sat}(T_0)$ and with the specific volume being that of the saturated liquid. In this case we find explicitly

$$G^2_{init} = \frac{\phi^2}{\left(c_L T - \phi\left[T\frac{dv_L}{dT} + v_L \right] \right)} \quad (24)$$

where $c_L=dh_L/dT$ is the liquid specific heat (modified as above by the heat-transfer term when appropriate). This constitutes a prediction of the initial mass ejection rate (per unit pipe area) which depends only on the initial temperature and the thermodynamic properties of the fluid in the pipe.

Numerical note: At the critical point dv_L/dT and $c_L = dh_L/dT$ are both singular but if we define the combined quantity

$$\psi \equiv \phi v_L - h_L$$

it appears that $d\psi/dT$ is finite everywhere. For numerical purposes close to the critical point it is convenient to recast these as

$$\left[v\left(\frac{d\phi}{dp} - 1\right) - \frac{d\psi}{dp} \right] G^2 = \phi \quad (25)$$

so that

$$G^2_{init} = \frac{\phi^2}{\left(v_L T\left[\frac{d\phi}{dT} - \frac{\phi}{T}\right] - T\frac{d\psi}{dT} \right)} \quad (26)$$

Allowance is made for heat transfer, as before, by making the replacement

$$\frac{d\psi}{dT} \rightarrow \frac{d\psi}{dT} - \frac{\rho_s}{\rho_L}\frac{4Y}{D}c_s$$

Evolution of the flow

Our quasi-steady model for the flow evolution in regime ii is as follows. We start with pure saturated liquid at T_0, p_0 and the initial flow rate defined above. The length of the two-phase zone, Zone 2 in Figure 1, is initially zero.

The flow rate will drop in time. Consider the situation when it has dropped to an arbitrary value G. The upstream pressure, temperature, and specific volume are unchanged. The new choke pressure can be computed from (23) with v(p) given by (18) and with a stagnation enthalpy

$$E = h_L(T_0) + G^2 v_L^2(T_0)/2 \qquad (27)$$

defined by the upstream end of Zone 2, and the exit pressure is then given by (15) and the flow will unchoke when G falls to a point where the choke pressure is atmospheric pressure. The volume profile with pressure (18) can be used in (20) to define the profiles in x. In particular (20) can be used to yield the distance to the point $(p_0,T_0,v_L(T_0))$ giving a prediction of the length L_2 of the two-phase zone when the given value of G is achieved.

Finally the total mass of fluid (per unit cross-sectional area) in the pipe is found from

$$M = \int_0^L \frac{dx}{v} = \frac{(L-L_2)}{v_l(T_0)} + \int_{p_e}^{p_0} \frac{dx}{dp}\frac{dp}{v} \qquad (28)$$

$$= \frac{(L-L_2)}{v_l(T_0)} + \frac{D}{2f}\left[-\left(\frac{1}{v_{L0}} - \frac{1}{v_e}\right) + \frac{1}{G^2}\int_{p_e}^{p_0}\frac{dp}{v^2}\right]$$

and the time taken to arrive at this value of G^2 can be evaluated from (10).

Let us note that this quasi steady approximation is formally justified as long as the liquid erosion velocity, dL_2/dt, which is of order $Gv_L(T_0)$, is much smaller than the fluid velocity Gv_e at the exit, that is to say as long as $v_e >> v_L$. For the most part this is satisfied well enough.

2.5 Flow in Regime iii - Further Evolution

The time-dependent flow problem

In the case of zero inflow the flash front will encounter the upstream end of the pipe and initiate regime iii. In regime iii the upstream pressure and temperature will also drop and the flow is intrinsically time-dependent, and so we start again from equations (6), (7) and (8).

Regime iii does not have the distinct liquid zone and in fact can be thought of as being in many ways very similar to the time-dependent single-phase gas pipeline problem analysed by Fanneløp and Ryhming (1982)[4] but with a rather different equation of state. It is therefore useful to follow the method of Fanneløp and Ryhming as far as possible in developing our regime iii model.

The method involves estimating the approximate profiles p(x,t), G(x,t) along the pipe, specified as given functions of x (but with unknown time dependence at this stage) to satisfy appropriate boundary conditions, using them to integrate the above equations over x, and obtaining ordinary differential equations in time, which can then be solved for the pressure and flow rates at the ends of the pipe. Encouragingly, Fanneløp and Ryhming showed that the results do not depend sensitively on the details of the chosen profiles.

Approximating the energy equation

In attempting this here, we rapidly discovered that there is one feature of single phase gas flow which gave Fanneløp and Ryhming an advantage that we do not share in the two-phase analysis. It turns out that the gas flow case can be considered isothermal - the temperature is approximately constant along the pipe. Fanneløp and Ryhming knew this from experience with actual gas pipelines, and in the course of this work we have now also found a formal mathematical

derivation of this. Essentially heat transfer into the fluid ensures that any temperature change (from a compressor) near the end is compensated by a return to ambient temperature within a finite distance. For a sufficiently long pipeline, then, the temperature variations occur over a very small fraction of the total length and contribute minimally to the profile integrals along the whole length of the pipe. The specific volume is simply proportional then to 1/p from the isothermal gas equation of state, and the energy equation reduces to $T=T_0$.

In the two phase case, not only is the form of v(p) rather more complicated, but the energy equation cannot reduce to anything like $T=T_0$. This last is very clear if homogeneous equilibrium holds (as indicated by Figure 3) as a pressure drop along the pipe *must* be accompanied by a temperature drop as $p=p_{sat}(T)$ holds at every point along the pipe.

If we are to make further progress with an analytic model of time-dependent two-phase flow, we first need an analogously simple approximation of the energy equation, but one which can support homogeneous equilibrium flow. The key to generalising the model of Fanneløp and Ryhming to two-phase flow is to observe that for gas flow, one might just has well have specified a constant specific enthalpy h. Because, for simple gases, h~T it makes no difference whether one chooses constant h or constant T. It makes a big difference for two phase flow however. And because the reason for the constant T is largely to do with heat transfer, then constant enthalpy is in fact a more physical way of thinking of it. We can adopt this uniform enthalpy hypothesis as an estimate of the behaviour of two-phase flow down long pipelines where any heat transfer may keep the overall specific enthalpy relatively constant along the pipe. In fact we'll go one step further and write

$$h + G^2 v^2 / 2 = E \qquad (29)$$

for some uniform E. This makes little difference compared with assuming uniform h as the velocity (Gv) term is generally small compared with h (except perhaps very close to a choke) especially by the time we're in régime iii, as by then the outlet velocity will have decreased very much from its initial value.

Adopting this equation also conveniently gives us (with the homogeneous equilibrium thermodynamics) exactly the same v(p) profile (18) as we had before, except that we are now considering that G may vary along the flow. However, consistently with the above remarks on the velocity terms in the simplified energy equation, we expect v(p) to be very close to its limiting ($G\rightarrow 0$) form throughout régime iii, and so any variation of G along the flow will make little difference to v(p).

For the same reason, in practice the stagnation enthalpy E varies only very slightly in time throughout régime ii, and so, consistently both with régime ii and with the gas flow analysis we shall take it to be constant in time through régime iii of the two-phase flow, and give it whatever value it adopts at the end of régime ii.

It is also important to note that h really is just the fluid enthalpy here. The arguments used in régime ii to include heat transfer by means of a pipe term added to the enthalpy only apply to quasi-steady flow and break down for fully time dependent flow. On the other hand we are allowing for heat transfer here as it is only the existence of heat transfer which allows us to argue for constant specific enthalpy in the gas flow case, and by extension for constant E here.

Approximating the momentum equation

Fannelop and Ryhming (1982)[4] neglect the $\partial G/\partial t$ in the momentum equation, arguing for a balance of pressure gradient and friction. With this approximation they integrate the momentum equation (7) along the length of the pipe. This gives

$$\int_{p_e}^{p_0} \left(1 + \frac{d(G^2 v)}{dp}\right) \frac{dp}{v} = \frac{2f}{D} \int_0^L G^2 dx \qquad (30)$$

The profile method can be illustrated by approximating the mass flux profile as

$$G^2 = G_0^2 + \left[G_e^2 - G_0^2\right] K(x/L) \qquad (31)$$

for some function K with K(0)=0, K(1)=1. And so the integral so the right hand side of (30) can be simply estimated. In fact we shall consider the case $G_0=0$ as being the only one of interest for régime iii and define k as the integral of K(z)dz from 0 to 1. The constant k will be of order 1.

It is worth noting in fact that Fannelop and Ryhming also neglected the $d(G^2v)/dp$ term on the left of the momentum equation. It tends to be small except near the choke and in the gas flow problem they were considering unchoked flow

for much of the time. We can do slightly better in the case of choked flow (and a relatively large range of specific volume) if we approximate

$$\frac{d(G^2 v)}{dp} \approx \lambda G_e^2 \frac{dv}{dp} \qquad (32)$$

with λ a constant of order 1. (Fannelop and Ryhming's approximation is recovered by setting λ=0.) With these approximations equation (30) reduces to

$$\frac{1}{G_e^2}\int_{p_e}^{p_0} \frac{dp}{v} - \lambda \ln\left(\frac{v_e}{v_0}\right) = 2kf\frac{L}{D} \qquad (33)$$

In principle the free constants k, λ reflect our lack of knowledge of the profiles. However, in practice we can demand that they be such as to make the results behave as continuously as possible through the transition from régime ii to régime iii. This effectively fixes k=1 and λ=1 and is consistent with assuming that changes in v along the pipe have much more important effect on the momentum balance than changes in G^2. It also means that the choke pressure may be estimated exactly as in régime ii.

The momentum equation now relates the two end pressures p_e and p_0 to the outflow G_e. We already have v(p) and so we can make use of it without any further profile assumptions.

However, as before, we need to know about v(p(x)) to evaluate the mass release rate and here an assumption about the pressure profile in x is required. Our first approximation followed the gas flow analysis exactly: we set p(x) to be quadratic in x with the appropriate values at the ends and dp/dx=0 at the closed upstream end. We discovered, however, that the isothermal gas equation of state v~1/p makes the mass integral uniquely tractable, and failed to make analytic progress to the same extent with our more complicated two-phase v(p). The maths gets complicated very rapidly here, which rather defeats the object of the approximation: choosing a "simple" profile to get results simply. Therefore, noting Fannelop and Ryhming's observation that the results are not strongly sensitive to the precise profiles chosen, it is worth asking if there is an appropriate choice which simplifies the calculation in this case.

In fact there is. Let us approximate the pressure profile p(x) by one which satisfies

$$\frac{d(\lambda G_e^2 v + p)}{dx} = -2kf\frac{G_e \mid G_e \mid v}{D} \qquad (34)$$

We don't have an explicit form for it and it only approximately satisfies dp/dx=0 at the closed end, but it does have the right values at each end as well as the correct analytic behaviour near the choke, and again it is very convenient in that it gives complete continuity of the mass integral (with the above values of k and λ) through the transition from regime ii to regime iii. With this profile, the mass integral is in fact

$$M = \int_0^L \frac{dx}{v} = \int_{p_e}^{p_0} \frac{dx}{dp}\frac{dp}{v} = \frac{D}{2kf}\left[-\lambda\left(\frac{1}{v_0}-\frac{1}{v_e}\right)+\frac{1}{G_e^2}\int_{p_e}^{p_0}\frac{dp}{v^2}\right] \qquad (35)$$

and can be evaluated as before from our knowledge of the specific volume profile v(p).

Evolution of the flow in régime iii

As earlier we can evolve the flow by decreasing the mass flux density G to a new value. The stagnation enthalpy E is assumed not to change. The exit pressure is computed exactly as in (15). Then (33) is solved for the new upstream pressure p_0, using the same volume profile v(p,G_e) as before. The mass of fluid in the pipe is given by the integral (35) and finally the time at which this new value of G is achieved is computed from (10) [with G_0=0].

This completes the main description of the model. It remains only to compare it with experimental data.

2.6 Thermodynamic and fluid dynamic properties

In order to evaluate solutions of the equations we need a number of thermodynamic properties of the fluid in the pipe.

2.6.1 Fluid dynamic properties

The required fluid-dynamic (as opposed to thermodynamic) parameter is the Fanning friction coefficient. Fannelop (1994)[7] p115 quotes a formula used by the American Gas Association:

$$\frac{1}{\sqrt{f}} = 4\log_{10}\left(\frac{3.7\,D}{z_0}\right) \qquad (36)$$

and recommends taking a roughness length for the inner pipe wall z_0=1.3 10^{-5}m (0.0005 inches) in the absence of any better information. Following this we estimate f=0.0029. (It turns out that the results - especially the mass release rate - are not enormously sensitive to this value and so we shall not, at this stage, explore further refinements.)

2.6.2 Thermodynamic properties

There is a choice of three different methods for determining thermodynamic properties which go under the names "Simple HEM", "DNV HEM", and "Hybrid HEM". They were developed in this order and will be described in this order below. The last is the recommended one, and has currently been made available only.

The Simple HEM

The Simple HEM is as follows. We approximate the liquid specific volume v_L as constant so that $dv_L/dT=0$. The liquid specific enthalpy is modelled as $h_L=c_LT$ with constant specific heat c_L. The vapour pressure curve is fitted in the appropriate range by the Clausius-Clapeyron form $p=Aexp(-B/T)$ so that $\phi=pB/T=pln(A/p)$. From these we can derive all the required properties.

For propane the values v_L=2.07 10^{-3} m^3/kg, c_L=2616 J/K/kg A=21244 bar, B=2299K provide a reasonable thermodynamic description in the region of interest. (These values have been extracted from, and in the case of the vapour pressure curve fitted to, correlations given by Reid, Prausnitz and Poling (1987)[6] and by Atkins (1994)[8].

The Simple HEM is not adequate for ethylene (or any other such substance) where the critical temperature is within a typical ambient range. It can, however, be used for well behaved substances which are not in the DNV database as long as the above properties can be estimated.

The DNV HEM

The DNV HEM is so named as it simply refers to the DNV property data base for all the properties it needs.

However this was found to be unacceptably slow. The main problem is that every time T(p) or v(T,p) are required, and these equations must be solved numerically.

The Hybrid HEM

To gain the optimum compromise between the speed of the Simple HEM and the general applicability of the DNV HEM the Hybrid HEM was developed. This must apply to ethylene and some of the features of its design reflect this. Problems with the critical point were solved by parametrising the initial mass flux according to (26) and this means that the independent correlations (along the saturation curve) were defined to be p(T) v_L(T) and ψ(T). The forms used are

$$p(T) = A\ \exp\left(\frac{-B}{T+C}\right) \qquad \text{(Antoine)} \qquad (37)$$

$$v_r(T_r) = 1 - \Lambda\,(1 - \alpha T_r)(1-T_r)^{1/3} \qquad (38)$$

where $T_r \equiv T/T_c$ and $v_r \equiv v/v_c$, and

$$\psi(T) = aT^2 + bT + c \qquad (39)$$

The substance is thus parametrised by the collection of 10 constants A, B, C, Λ, α, T_c, v_c, a, b, c. The derived proprties are

$$T(p) = \frac{B}{\ln(A/p)} - C \quad (40)$$

$$\phi \equiv T\frac{dp}{dT} = pT\frac{d\ln(p)}{dT} = \frac{BpT}{(T+C)^2} \quad (41)$$

$$\frac{d\phi}{dT} = \frac{\phi}{T}\left[\frac{\phi}{p} - \frac{T-C}{T+C}\right] \quad (42)$$

$$\frac{dv_L}{dT} = \frac{v_c}{T_c}\frac{dv_r}{dT_r} = \frac{v_c}{T_c}\left[\frac{1}{3}\Lambda(1-T_r)^{-2/3}\left[(1-\alpha) + 4\alpha(1-T_r)\right]\right] \quad (43)$$

$$\frac{dv_L}{dp} = \frac{dT}{dp}\frac{dv_L}{dT} = \frac{T}{\phi}\frac{dv_L}{dT} \quad (44)$$

$$\frac{d\psi}{dT} = 2aT + b \quad (45)$$

$$h_L(T) = \phi(T).v_l(T) - \psi(T) \quad (46)$$

$$\frac{dh_L}{dT} = \phi\frac{dv_l}{dT} + v_l\frac{d\phi}{dT} - \frac{d\psi}{dT} \quad (47)$$

$$\frac{dh_L}{dp} = \frac{T}{\phi}\frac{dh_l}{dT} \quad (48)$$

all of which can be evaluated much more rapidly than consulting the database.

The independent correlations (37), (38), (39) are found by demanding agreement with the database functions at two or thee points in the relevant range: the maximum temperature is the initial temperature and the minimum temperature is the ambient pressure boiling point. The following graphs illustrate the accuracy of these correlations for propane and ethylene.

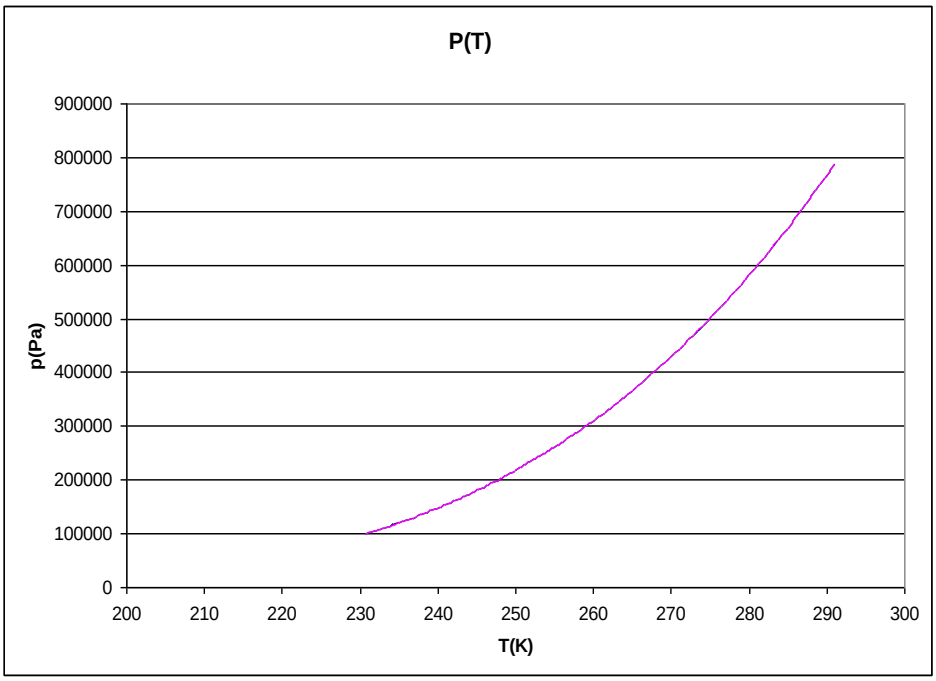

Figure 4. The vapour pressure curve for propane

The correlation used by the Hybrid model is superimposed on the database correlation from which it was derived. To the naked eye, they are indistinguishable on this graph.

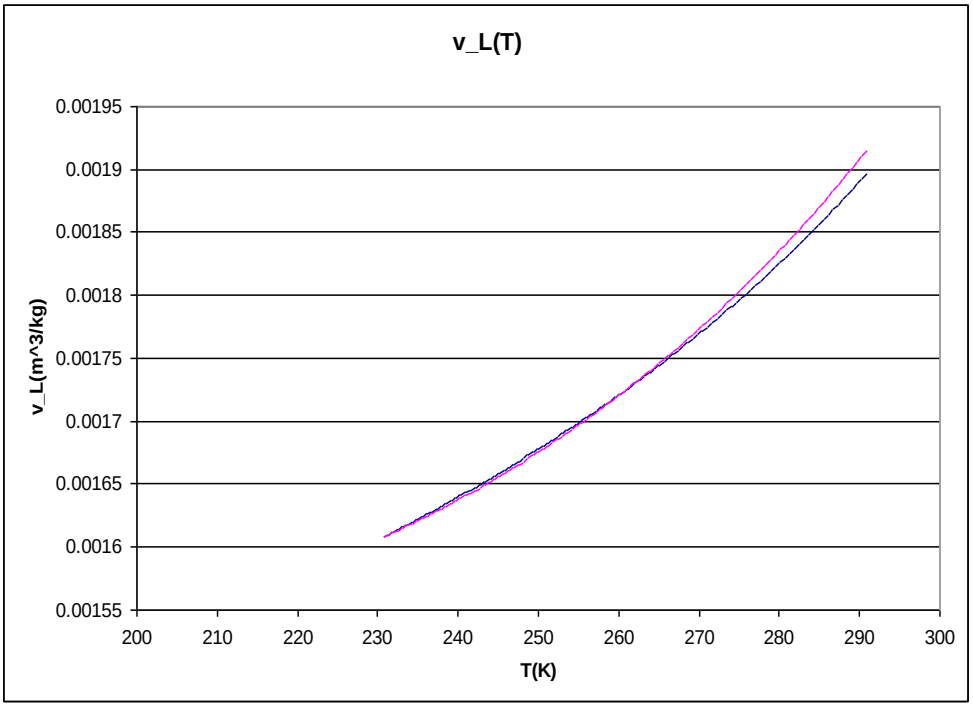

Figure 5. The liquid specific volume for propane

The correlation used by the Hybrid model is superimposed on the database correlation from which it was derived. The suppressed zero on the vertical axis means that they are very close.

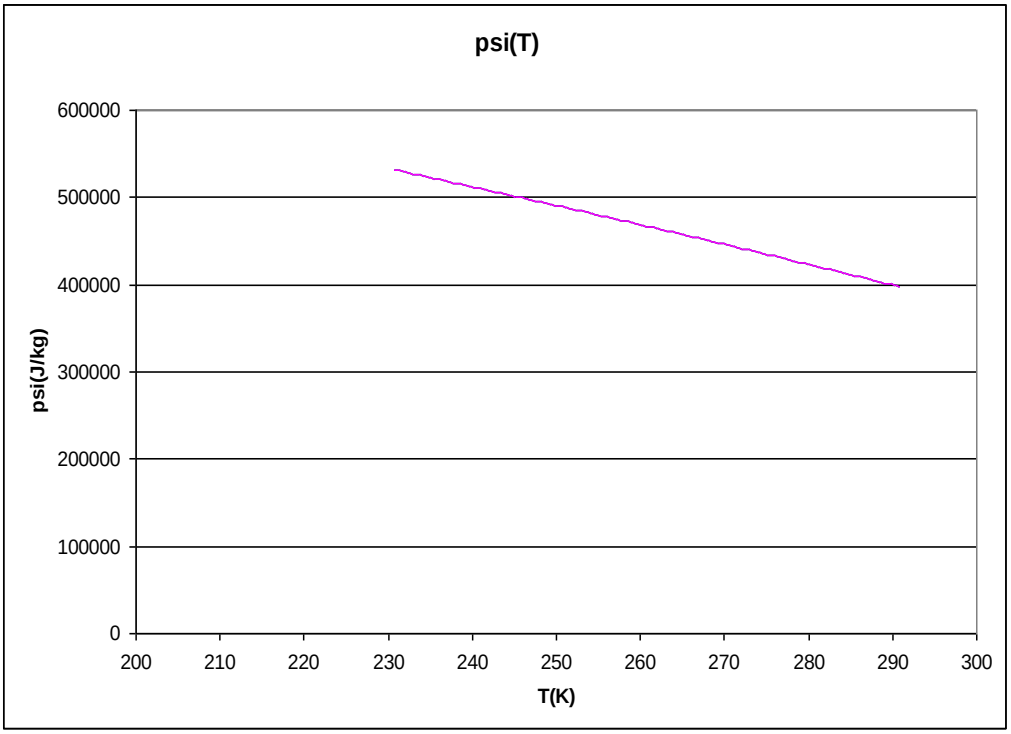

Figure 6. The function ψ(T) for propane

The correlation used by the Hybrid model is superimposed on the database value from which it was derived. To the naked eye, they are indistinguishable on this graph.

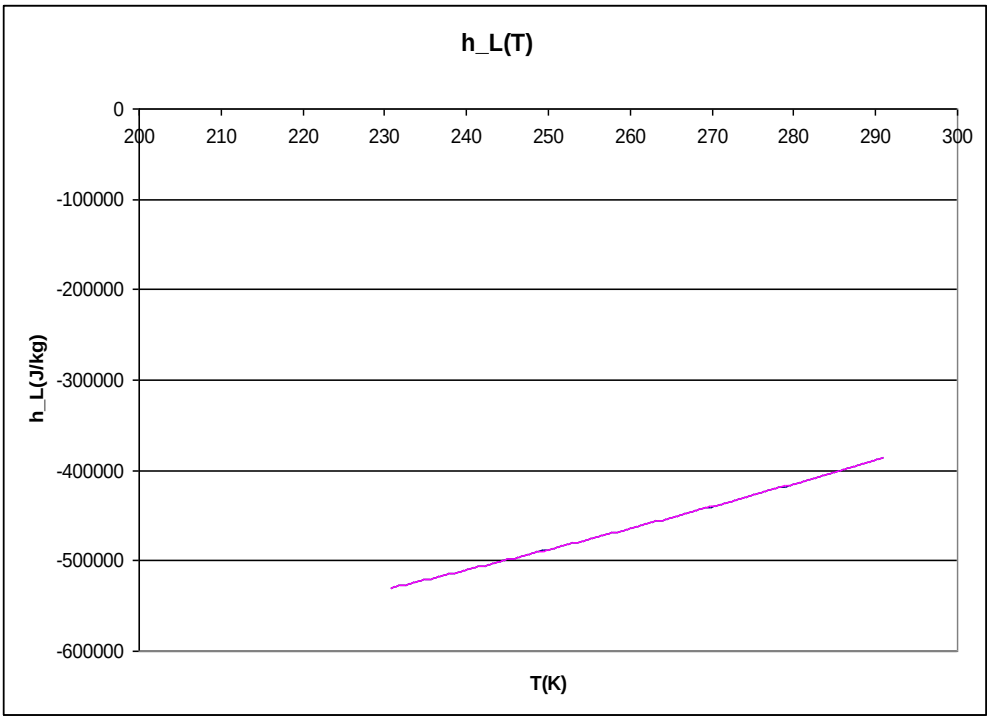

Figure 7. The liquid specific enthalpy of propane (derived from ψ(T))

The correlation used by the Hybrid model is superimposed on the database value from which it was derived. To the naked eye, they are indistinguishable on this graph.

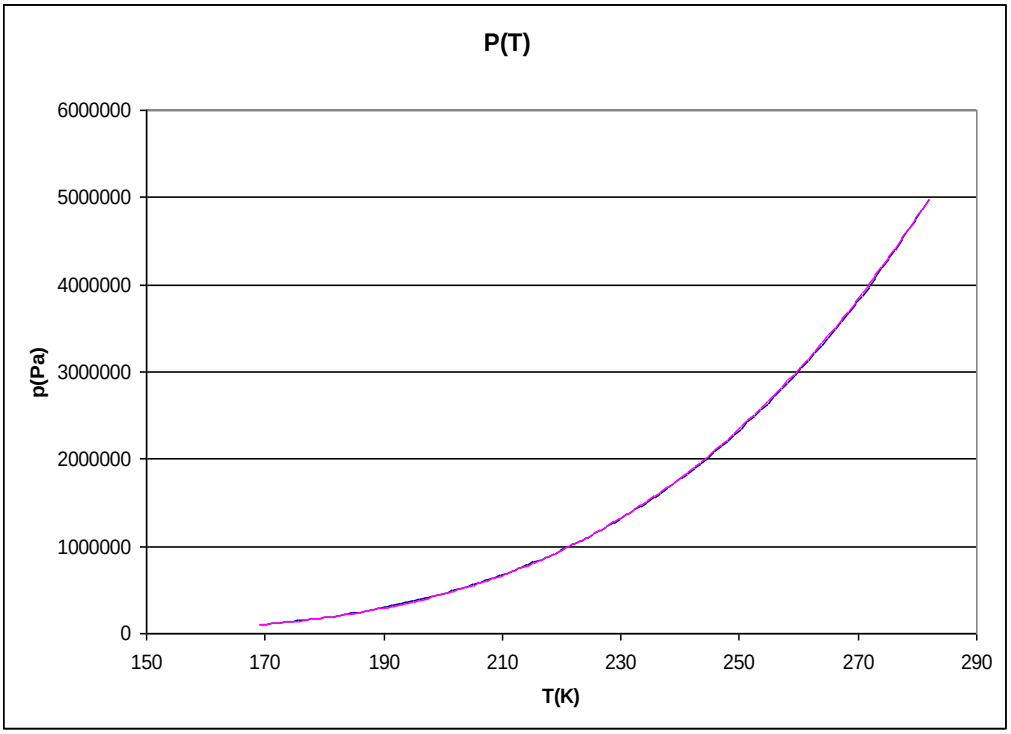

Figure 8. The vapour pressure curve for ethylene

The correlation used by the Hybrid model is superimposed on the database correlation from which it was derived. To the naked eye, they are indistinguishable on this graph.

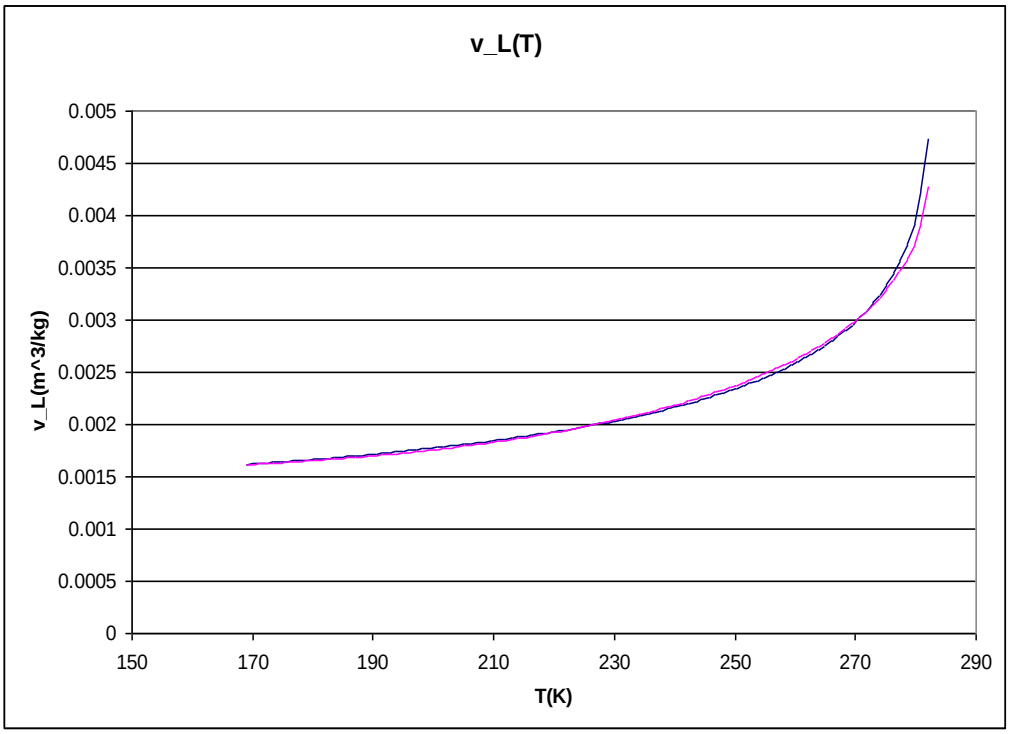

Figure 9. The liquid specific volume for ethylene

The correlation used by the Hybrid model is superimposed on the database correlation from which it was derived. The correlation works well all the way to the critical point (282.3K) where v_L is finite but dv_L/dT is infinite.

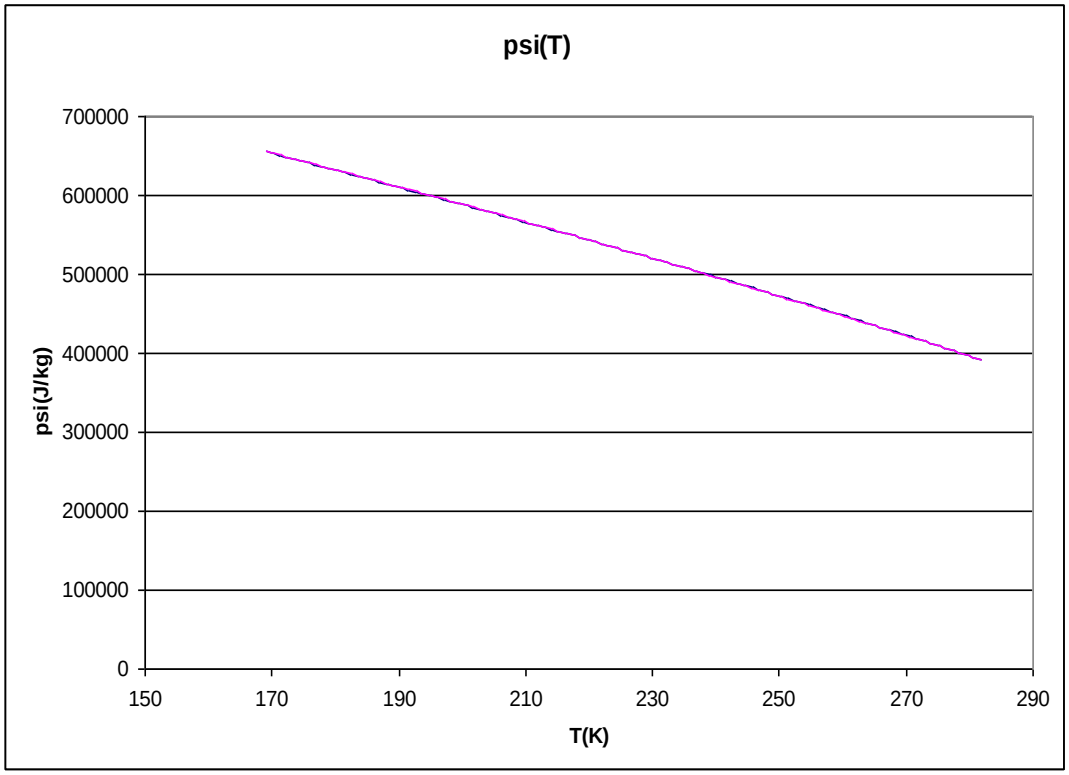

Figure 10. The function ψ(T) for ethylene

The correlation used by the Hybrid model is superimposed on the database value from which it was derived. To the naked eye, they are indistinguishable on this graph.

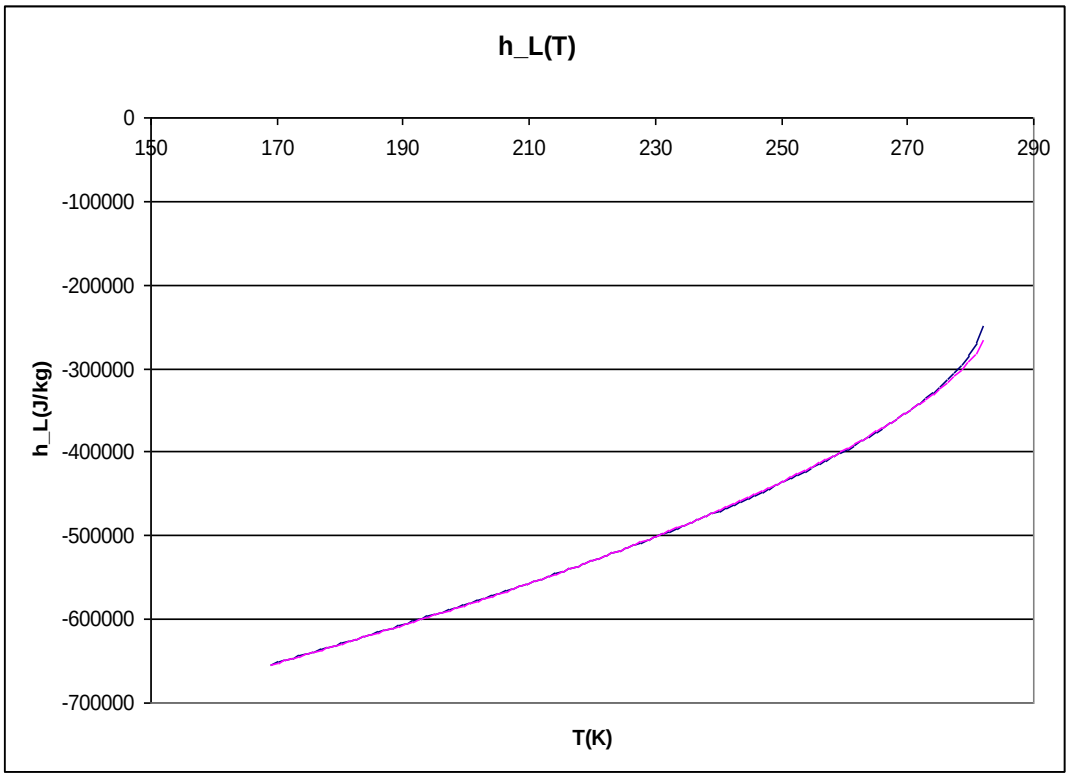

Figure 11. The liquid specific enthalpy for ethylene

The correlation used by the Hybrid model is superimposed on the database correlation from which it was derived. The correlation works well all the way to the critical point (282.3K) where h_L is finite but dh_L/dT is infinite.

2.7 Initial Comparison with the Isle of Grain Trials

We are now in a position to compare the model with the Isle of Grain experiments. We shall examine first the full bore rupture of a 6 inch pipe - trial P42. Our comparisons with the pressure and temperature at each end of the pipe, and with the evolution of the mass inventory are shown in
Figure 12,
Figure 13 and Figure 14. We emphasise that we have adjusted no free parameters to achieve the fit: thermodynamic properties of propane have been taken from books, as was the Fanning friction coefficient. Other possible parameters k and λ were fixed to achieve continuity from régime ii to régime iii as described above.

The pressure and temperature data at the closed end of the pipe are very suggestive of our régimes ii and iii, as they remain approximately constant and then start to drop at a time which matches our prediction fairly closely - especially in the pressure curve.

We have shown predictions including our heat transfer model in régime ii (bold lines) and with it switched off (thinner lines). Including the heat transfer improves the fit.

We note from the data that the open end pressure drops to around 0.5bar at the end which we regard as indicating a 0.5bar or so error on the pressure data, in view of which we believe our predictions to be very reasonable.

Temperature changes in the data take slightly longer than our model predicts and we can speculate that this may be attributable to the way in which temperature was measured. We emphasise however that the fits to pressure and temperature data are constrained in our model by the homogeneous equilibrium approximation, which we believe to be strongly justified by the overall data (Figure 3).

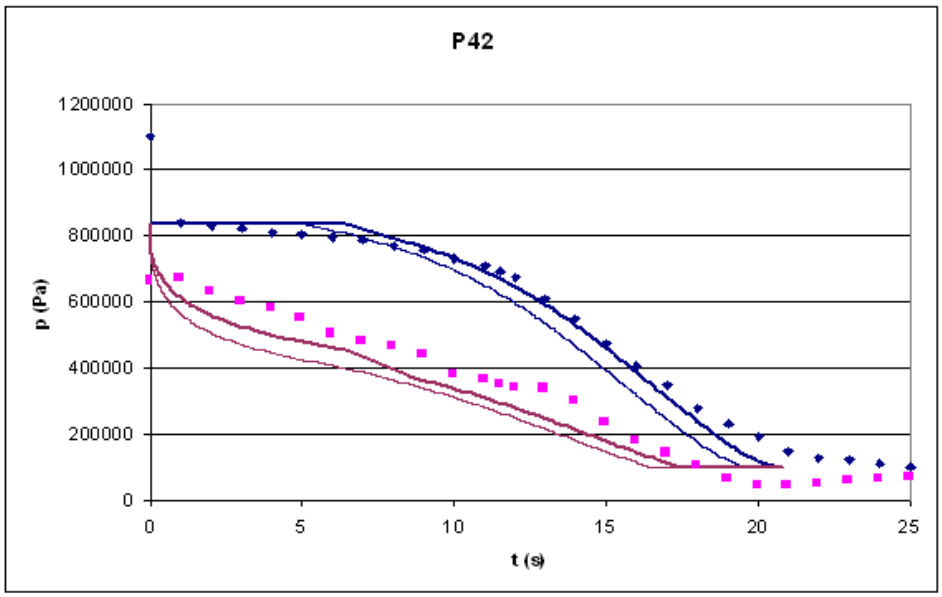

Figure 12. PIPEBREAK pressure predictions for Isle of Grain Trial P42
The measured values of the pressure at the open (squares) and closed (diamonds) ends of the pipe. The lines are the model predictions with heat transfer (thick lines) and without (thin).

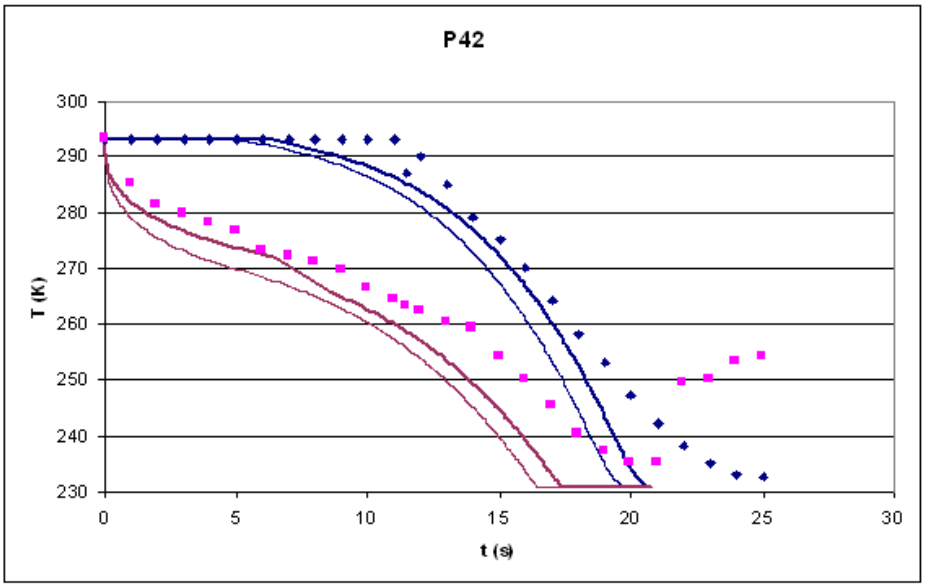

Figure 13. PIPEBREAK temperature predictions for Isle of Grain Trial P42
The measured values of the temperature at the open (squares) and closed (diamonds) ends of the pipe. The lines are the model predictions with heat transfer (thick lines) and without (thin).

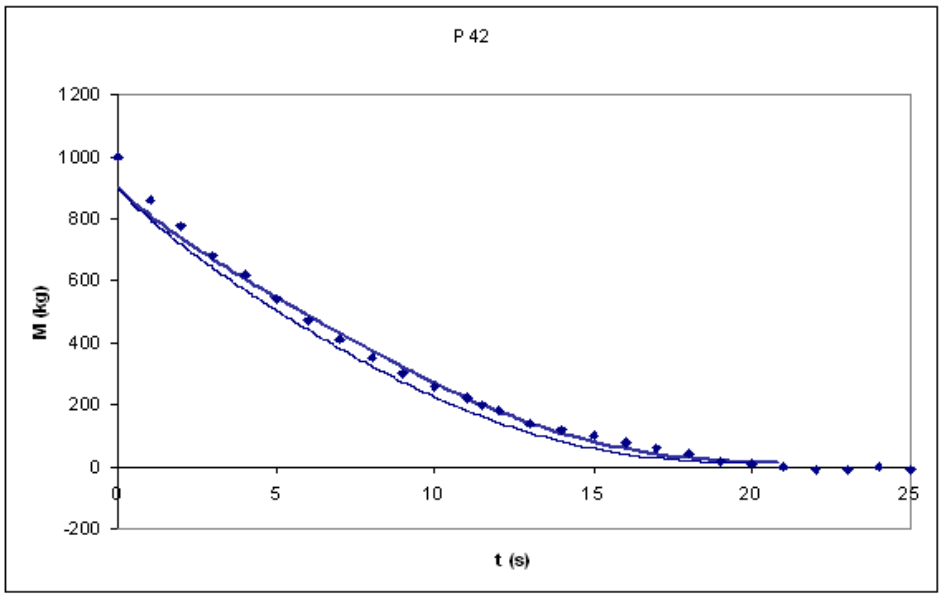

Figure 14. PIPEBREAK predictions of the mass content of the pipe for Isle of Grain Trial P42
The measured values of the mass content of the pipe are indicated by the points. The lines are the model predictions with heat transfer (thick lines) and without (thin).

One of the quantities of prime interest, the time taken to empty the pipe completely, is predicted very accurately and appears to be quite insensitive either to detailed assumptions about heat transfer, or to the precise value of the Fanning friction coefficient.

Although we regard these predictions as eminently acceptable, especially considering that we adjusted no free parameters, it is interesting to think how one might make them even better. In fact this looks difficult. It would be nice if our initial mass release rate were slightly steeper. However this is predicted absolutely from the thermodynamic properties of propane and does not depend on anything else (and in particular it does not depend on the Fanning friction coefficient at all). Allowing for a small positive dv_L/dT might increase it slightly and we'll find out when we couple in the more sophisticated thermodynamic model, but we don't expect a big effect. Otherwise, looking at régime ii where our prediction of the upstream pressure will not change, it seems we need a slightly higher downstream pressure and a slightly higher mass release rate to make any improvement in the fit. We have already argued that adjusting the friction coefficient will

not achieve this (in the early stages) and therefore it is difficult to see how we can get mass out of the pipe faster with an overall smaller pressure gradient. In fact the predictions appear remarkably stable to any small adjustment we might have the freedom to make. This is already evident in the relatively small difference made when one allows for, or neglects, heat transfer. A slightly higher value of the Fanning friction coefficient may slightly improve the pressure and temperature curves at later times, but may also make the overall mass curve slightly worse, and so we are content, for the moment, to leave it at the prescribed value.

We regard the above comparison as a successful demonstration of the concepts, and will show further data comparisons later in this manual.

2.8 Discussion and Conclusions

We have presented a one-dimensional model of two-phase fluid flow down a pipe following an accidental full-bore breach. It is applicable to pipelines containing fluids with a normal boiling point below ambient temperature.

We have used a quasi-steady flow model for the movement of flash front into the fluid, followed by a generalisation of the method developed by Fannelop and Ryhming (1982) for long gas pipelines. The resultant model predicts the evolution of the system including the mass flux out of the breach with essentially no unknown free parameters. Comparisons done thus far with the Shell Isle of Grain experiments are extremely encouraging.

The model has points in common with both the gas pipeline model of Fannelop and Ryhming and with the model expounded in various papers by Leung and co-workers - for example Leung (1986)[5]. An interesting point of comparison is the variation of specific volume with pressure along the pipe. In those two models and the current one, the solution method is essentially to derive v(p) from a combination of the energy equation and the equation of state (or guess it) and then use it in the momentum equation to relate the upstream and downstream pressures to the release rate. As noted above, Fannelop and Ryhming have an isothermal gas approximation so that v=b/p for some constant b. Leung's two-phase model uses the form v=a+b/p with constants a and b, which are chosen to optimise this form at and near the high pressure end of the pipe. The current model derives v(p) from the energy equation and the homeogeneous equilibrium model of state, and the result in fact also depends on the mass flux v(p,G^2) although the G^2 dpendence may not always be strong and will diminish with time. But even at small G^2 the specific volume turns out to have a more complicated dependence on p than can be accomodated by Leung's approximation, and we therefore believe our model to be much more appropriate when the pressure difference between the ends of the pipe is more than a factor of two or so. Also our model, via its function v(p,G^2) actually predicts the choke pressure, something which must be done separately if a simpler approximate form is used.

Richardson and Saville (1996)[3] have an apparently much more complex model which accounts for mixtures of hydrocarbons, something which they imply is important for understanding the flow in the Isle of Grain experiments. In contrast we find that a very much simplified model (both dynamically and thermodynamically) is capable of yielding excellent results. In fact if we examine Richardson and Saville's fit to the Isle of Grain trial discussed above, we see no better a fit to the data than is given by our own model. This may provide added support for our conclusion that it is difficult to improve the fit to the mass and pressure curves simultaneously, but in any event we conclude that the accuracy of our model is very comparable with that of the more complex model of Richardson and Saville.

2.9 Smaller breaches

Let us now generalise the model to allow for smaller breaches (but not very small) continuing for the moment to consider the breach to be at the end of the pipe.

Suppose that the area of the orifice is A_x with A_x<A. We define a dimensionless "aperture" α (≤1) by

$$A_x = \alpha A \qquad (49)$$

and a mass flux density G_x in the orifice

$$G_x = G/\alpha \qquad (50)$$

so that the total mass flux through the orifice is

$$G_x A_x = GA \qquad (51)$$

Here G may be thought of as the mass flux density immediately behind the orifice; we shall denote it as the "exit mass flux density" as this is a particularly useful quantity with which to generalise the full-bore rupture model. The quantity G_x will be denoted the "orifice mass flux density".

Similarly if the specific volume immediately behind, and in, the orifice is v, then we shall denote

$$w = Gv \qquad (52)$$

as the "exit velocity" (immediately upstream of the orifice) and

$$w_x = G_x v \qquad (53)$$

as the orifice velocity - that with which the fluid emerges into the open.

Apart from this mass flux conservation in the orifice the principal effect of the orifice in the model is to redetermint the choke pressure to a value appropriate for mass flux density G_x and velocity w_x through an area A_x. Accordingly we define the exit (and orifice) pressure to be

$$p_e = \max(p_a, p_{choke}(G/\alpha)) \qquad (54)$$

in place of (15). It is implicit in the model that the breach is not too small. For a sufficiently small breach, the pipe will no longer behave as a pipe (i.e. with one-dimensional flow) and one may expect resistance at the orifice, and not just a modified choke pressure to be important. These effects are outside the scope of the model.

2.10 The computational procedure

The above equations are most conveniently solved by the following computational procedure.

First compute the initial value of G in regime ii by demanding that the choke pressure is equal to the initial pressure (which is the saturation pressure at the initial temperature). Compute the mass of fluid in the pipe from a knowledge of the liquid specific volume.

Decide how many steps *n* are to be made and evolve the flow by decreasing G by $(G_{initial}-G_{inflow})/n$ at each step (as ultimately G will tend to G_{inflow} if the flow is arrested in regime ii or to zero if $G_{inflow}=0$). Then iterate the steps which may be described broadly as:

1. Decrease G to the next value
2. evaluate the exit pressure $p_e(G_A)$ as the maximum of the choke pressure and ambient
3. compute the length of the two-phase zone (regime ii) or the upstream pressure (regime iii).
4. complete the computation of the state of the fluid the up- and downstream ends of the two-phase flow
5. compute the mass of fluid in the pipe.
6. compute the time at which the above will be achieved.

This provides the evolution of the flow in equally decreasing steps of G rather than at equal time steps.

2.11 ATEX model for atmospheric expansion

In the case of the presence of choked flow, immediately outside the breach orifice atmospheric expansion takes place from the choked pressure to the ambient pressure. This results in flashing of the liquid (reduced liquid mass fractions), increased velocities, and droplet atomisation. The post-flash temperature will be equal to the saturated liquid temperature at the ambient pressure.

The atmospheric-expansion model ATEX is invoked in GASPIPE to calculate the post-expansion data (velocity, liquid mass fraction, droplet diameter) from the pre-expansion data. This is carried out for each time. See the ATEX theory manual[9] for full details on the ATEX model.

3 A BREACH AT SOME POINT ALONG THE PIPE

3.1 Introduction

If the breach is at some arbitrary point along the pipe, we shall consider the pipe in two *branches*: Branch A from the original upstream end of the pipe to the breach, and Branch B from the original downstream end of the pipe to the breach.

The model already described will be considered to apply to both branches (with possible modifications below) and, in particular, after the initial depressurisation regime, the flow in each branches will be considered to be towards the breach.

We identify two possibilities.

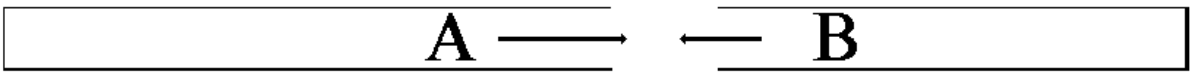

Figure 15. A disjoint break (default model). 'A' and 'B' label the 'branches' of the resultant pipe.

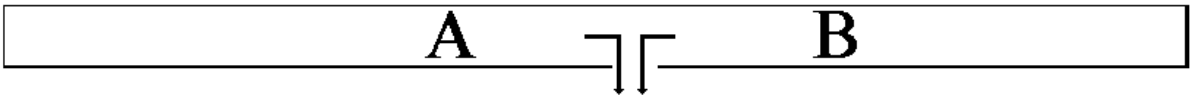

Figure 16. An interacting break. 'A' and 'B' label the 'branches' of the resultant pipe.

Disjoint flow
The first is that, for a full bore rupture, the pipe may be completely split apart (a catastrophic guillotine break). This defines two independent branches each behaving as already described and, for the purposes of flow computation, knowing nothing about the existence of the other branch. The above model can be used independently in each case and the results for the mass release rate may be added (for example if mixing of the two jets is assumed to take place in a crater around the breach) or treated separately if two jets in different directions are to be considered.

It is also convenient to consider the possibility (whether or not it may seem unlikely *a priori*) that in the formation of such a split the open ends of the pipe might be "crimped" each to an orifice area $A_x=\alpha A$. Then each branch my be considered independently with now with the same reduced orifice area. We shall discuss the advantages of this below. (It may be possible that each obtains a different orifice area, but the model is sufficiently complicated with a single aperture parameter α, which will be adequate for our purposes below. We therefore only consider the case of equal orifices.)

This model is currently applied as default in PIPEBREAK and is further described later on in this section.

Interacting flow
The second, more complicated, possibility is that the pipe does not entirely split apart but that a hole is formed so that the flows from the two branches interact at the orifice.

In this case it is convenient to define the area of the orifice as $2A_x$ again with $A_x = \alpha A$ with $\alpha \leq 1$. This definition makes it straightforward to compare with the disjoint flow case.

In the model we shall consider what happens in the interaction in two stages. First we shall consider the flows down two branches, each of area A, to combine into a single "effective flow" of cross-section 2A. Then we shall consider what happens to that effective flow when the cross-section narrows by a factor α in the aperture.

This model is described in full detail in 7. This model has been implemented in PIPEBREAK. Since further work is required, it is not recommended to be used by the user and the option of disjoint flow should be used always.

3.2 Combining branch contributions

For purpose of subsequent dispersion calculations, the contributions of the upstream branch A and the down-stream branch B need to be combined to obtain the total or averaged contribution (as input to the dispersion calculations).

The pipe is assumed to be split into two branches A,B with identical breach areas A_{breach} = min(A, A_{hole}/2) = α A, where A_{hole} is the total leak area and α the relative aperture of the breach. For combining the branch contributions, PIPEBREAK considers the two branches as "coalescing" at a "total exit" of area 2*A immediately behind an effective orifice area of 2 A_{breach} = 2*α*A. Herewith it is assumed that both branches point in the same direction. The post-expansion discharge results for each branch are combined to obtain the total discharge data. Conservation of total mass, liquid mass and momentum is applied to calculate the total (averaged) discharge data: total flow rate, averaged liquid mass fraction, averaged velocity, and averaged droplet size diameter.

The above approach is simplistic and approximate. In the real life, the branches may point in different directions. For smaller leaks (for which PIPEBREAK is less accurate anyway), the averaging of branches may be more appropriate prior to the expansion rather than after the expansion.

The precise equations adopted for the above approach are given below:

Total mass rate

The total mass rate G_T (kg/s) is obtained from imposing mass conservation, i.e. by summing of the mass rates G_A, G_B for both branches A and branch B

$$G_T = G_A + G_B \qquad (55)$$

Averaged post-expansion velocity

The averaged post-expansion velocity w_T (m/s) is obtained from momentum conservation, i.e. from mass-rate averaging of the post-expansion velocities w_A,w_B for both branches A and B:

$$w_T = \frac{G_A w_A + G_B w_B}{G_A + G_B} \qquad (56)$$

Averaged post-flash liquid mass fraction

The averaged post-flash liquid mass fraction y_T (-) is obtained from conservation of liquid mass, i.e. from mass averaging of the post-flash liquid mass fractions y_A, y_B for both branches A and B:

$$y_T = \frac{G_A y_A + G_B y_B}{G_A + G_B} \qquad (57)$$

Averaged post-flash SMD diameter

The definition of the Sauter Mean Diameter is as follows:

$$D = d_{32} = \frac{\mu_3}{\mu_2}, \quad with \quad \mu_m = \int_0^\infty {d_p}^m f(d_p) d(d_p) \qquad (58)$$

where $f(d_p)$ is the probability droplet distribution for the droplet diameter d_p ($0 < d_p < \infty$). From the above definition for μ_3, it follows that the total liquid mass rate (kg/s) is given by

$$G^L = y\ G = N\,\rho_{sat}(p_a)\int_0^{\infty}\left[\frac{4}{3}\pi\left(\frac{d_p}{2}\right)^3\right]f(d_p)d(d_p) = N\,\rho_{sat}(p_a)\frac{\pi}{6}\mu_3 \qquad (59)$$

where N is the total number of droplets / sec and $\rho_{sat}(p_a)$ is the post-flash saturated liquid density.

The total distribution function $f_T(d_p)$ and the 'total' SMD droplet diameter D_T can be expressed in terms of the corresponding branch data as follows:

$$f_T(d_p) = \frac{N_A f_A(d_p) + N_B f_B(d_p)}{N_A + N_B}\ , \qquad \frac{1}{D_T} = \frac{N_A\mu_{2A} + N_B\mu_{2B}}{N_A\mu_{3A} + N_B\mu_{3B}} \qquad (60)$$

Using Equation (59) into Equation (60), it can now be shown that the inverse of the averaged post-flash SMD diameter, $1/D_T$, is obtained from liquid-mass averaging of the inverse of the post-flash diameters $1/D_A$, $1/D_B$ for both branches A,B. Thus

$$\frac{1}{D_T} = \frac{\frac{y_A G_A}{D_A} + \frac{y_B G_B}{D_B}}{y_A G_A + y_B G_B} \qquad (61)$$

4 VALVE OPERATION

4.1 Introduction

In a risk assessment we may wish to consider the effects of the natural reaction of the pipeline operators (or of automated systems) in response to an accident - closing the pipeline off by means of valves.

We therefore consider that at one or more specified points along the pipeline there are valves, and that these may be closed instantaneously (and independently) at any time. The section of a branch of the pipeline (defined earlier) between the breach and the nearest closed valve will be denoted the "active" zone. When a valve closes any fluid outside of the newly diminished active zone is considered to be trapped and plays no part in further computations.

Apart from that, if a valve closes in a branch where there is an inflow, than that inflow is thereafter considered to have terminated as new fluid can then no longer reach the active zone.

4.2 Re-initialisation on valve closure

When a valve closes it can be in various locations with respect to the flow. We know the postulated breach location and we know the valve location, and so we can immediately determine which Branch it is in. But depending on the time of closure, different procedures must be adopted to assess its effect on the flow.

4.2.1 Closure of a valve outside the active zone

If a valve closes in a part of the branch which is already isolated (by an earlier valve closure) from the active zone, then it has no effect.

4.2.2 Closure of a valve in regime ii, zone 1

If at the time a valve closes the flow is in regime ii and if the valve closes in the saturated liquid zone (1) upstream of the flash front, then the effect is simply to shorten the active zone and trap a section of saturated liquid. The two-phase flowing zone and motion of the flash front are not immediately affected (although the transition to regime iii will now be as soon as the flash front encounters the nearest closed valve and so the later flow will be affected).

4.2.3 Closure of a valve in regime iii or in regime ii zone 2

These possibilities both correspond to a valve closure in a flashing two-phase zone. The pressure at the valve closure point is assumed unaffected, and the flow in the new active zone is assumed identical to what it was in that part of the previous active zone. Fluid upstream of the closure is trapped.

If the valve closes on regime iii, then a shortened regime iii results with a correspondingly smaller pressure drop across the new, shorter active zone, than was present in the old, longer active zone. If the valve closes on regime ii zone1, then the new active section now contains no saturated liquid zone and the flow is automatically forced into a regime iii flow.

4.3 Summary

In each case there on valve closure, is no immediate change in the outflow, but later the flow will be different - as there is now less fluid which can escape and sometimes there is (immediately) a smaller pressure drop driving it.

5 VALIDATION

5.1 Introduction

Above we showed a comparison of the model results with Isle of Grain trial P42 - a full bore rupture of a 6" pipe. The following figures show the comparison of the model with the other Isle of Grain trials. The configurations were as follows:

Trial	Inner diameter	Size of breach (% pipe cross-section)	Initial Temperature
P40	154mm	100%	291K
P42	154mm	100%	293K
P45	154mm	23.72%	289K
P47	154mm	10.54%	288K
P61	52mm	100%	(?)
P63	52mm	45.3%	292K
P65	52mm	100%	297K
P66	52mm	45.3%	286K

In trial P66 the aperture was an equilateral triangle; in all other cases it was circular. In each case the model was run with no adjustment of parameters other than those in the table which define the experiment.

5.2 Discussion

5.2.1 Full bore rupture

The full bore breach trials P40, P42, P61, and P65 exhibit excellent agreement of the evolution of the mass of fluid in the pipe (and hence of the main quantity of interest - the release rate). The model accurately predicts the longer release times from the narrower pipe.

The agreement of the evolution of the upstream and downstream pressure and temperature is also quite reasonable in these trials (except for the downstream measurements in trial P61 where the experiment clearly failed).

P65 illustrates the sort of problems one faces in trying to better. The mass release prediction is as near perfect as one could wish. In the early stage, our regime ii, the upstream temperature is well predicted but the pressure less well so. No homogeneous equilibrium model could therefore do any better. And yet the homogeneous equilibrium assumption brings about such an immense simplification in the physics, and seems to do so well overall that we would argue strongly that it should not be abandoned. But then in regime iii our upstream prediction falls off a little too rapidly. The down-stream prediction in this case is accurate to within the errors implicitly indicated in the data by the late time pressure measurements which should surely be at 1 bar. And of course it is always possible that the temperature measurements upstream lagged a little behind the temperature changes in the actual fluid.

5.2.2 45% aperture - trials P63 and P66

These trials have the next smaller aperture in percentage terms. The mass release prediction is still excellent (especially in view of the fact that the model has no free parameters). Again the reduction in aperture causes slightly longer release times. But under-prediction of pressure and temperature in the regime iii model is more noticeable here than in the full bore releases. We'll discuss that below.

5.2.3 24% and 11% aperture - trials P45 and P47

In the 24% aperture case (trial P45) the mass release prediction is less good, and in the 11% case (P47) it is poorer still - although still only under-predicting the overall release time by of order 30%. But the pressure and temperature traces are revealing. The measured pressure difference along the pipe is very small and it is difficult to believe that what we are seeing is a one-dimensional flow being driven by pressure gradients along the pipe. It is reasonable to suppose that the pipe acts more like a vessel in this case and that the one dimensional assumptions of our model are out of place here.

The model itself is trying to tell us something in the regime ii is very brief in P45 and even briefer in P47 - the flash front traverses the whole pipe very quickly, in what looks like an attempt to equilibrate the situation as rapidly as possible.

5.2.4 The mass release rate

It is interesting to note that the mass release rate is better predicted in all cases than the pressures and temperatures. This may partly be because it could be measured more accurately. However it correlates with the observation that the pressure difference along the pipe is much better predicted than the end pressures themselves. It may therefore be that our flow model is rather better than the prediction of the choke pressure (which gives our exit pressure prediction most of the time - everywhere where the exit pressure is above 1 bar). We conclude tentatively that the choke pressure prediction may be a little simplistic. There are certainly grounds for believing that the exit pressure model may not be the whole story for small apertures (as the flow cannot be entirely one-dimensional in a constricted out-flow).

5.2.5 Richardson and Saville's predictions

Richardson and Saville also admit to problems fitting the partial breach data. In order to do so they had to assume a discharge coefficient of 0.8 and rather larger effective orifices for trials P45, P47, P63, and P66, although their precise procedure is not explained. They point out that it is not entirely understood why this is necessary.

In our case increasing the orifice diameter for a given total mass flux would decrease G through the orifice and hence require an decrease in choke pressure. There will be some compensation as this feeds back to increase the mass flux but in general we expect lower exit pressure. Except in trial P47 (the smallest relative orifice) this would not seem to be beneficial to our predictions of pressure, and experience suggests the efflux rates (the reason R&S quote for adopting different exit conditions) would be less affected.

5.2.6 Conclusion

There are good reasons to suppose that our model is not appropriate for very small breaches. The mass release rates and pressure difference along the pipes appear to be well predicted for breaches down to of order 50% area aperture, but below this size the model should be used only with caution (which should be progressively more extreme as one considers smaller breaches).

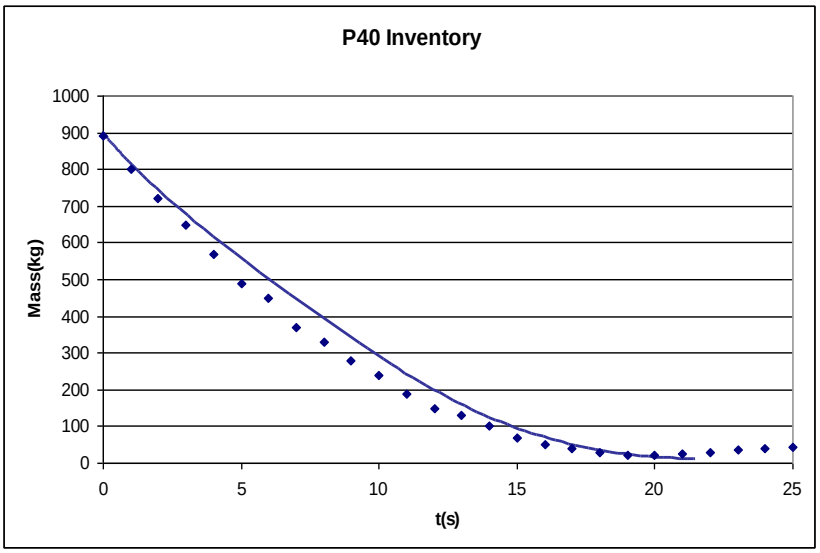
P40 Inventory
Mass(kg)
1000
900
800
700
600
500
400
300
200
100
0
0
5
10
15
20
25
t(s)

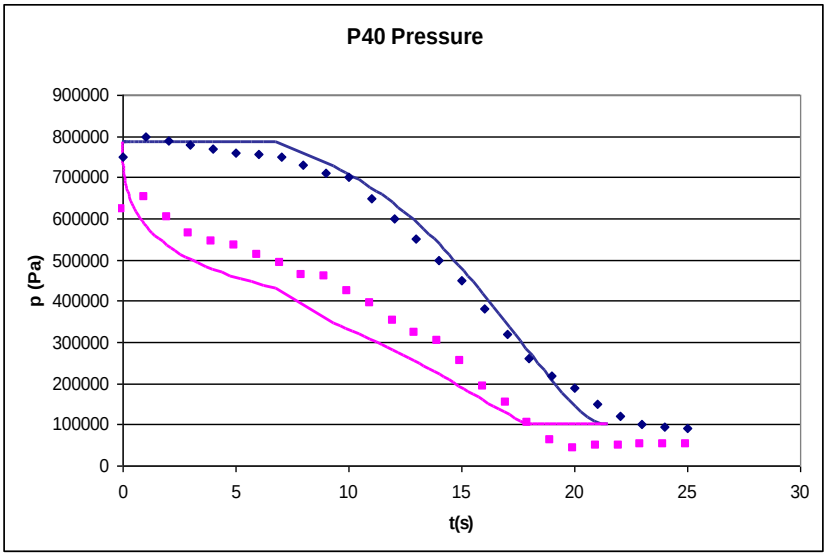
P40 Pressure
p (Pa)
900000
800000
700000
600000
500000
400000
300000
200000
100000
0
0
5
10
15
20
25
30
t(s)

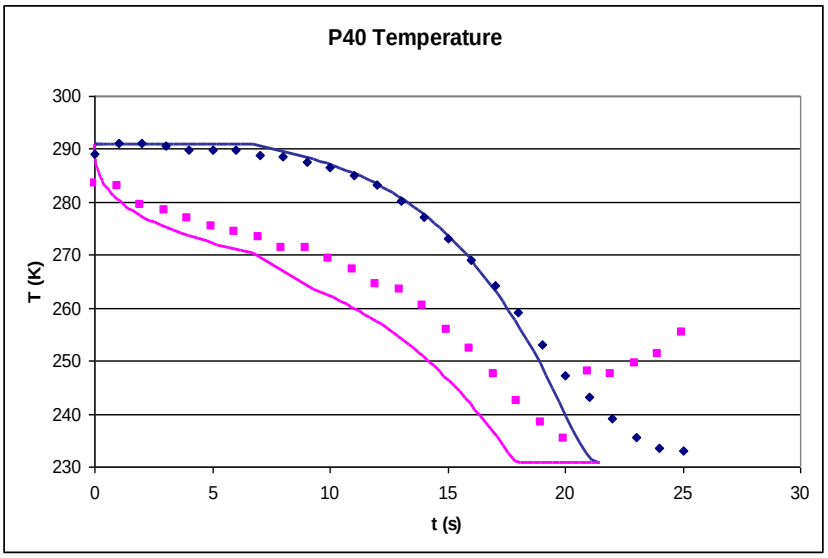
P40 Temperature
T (K)
300
290
280
270
260
250
240
230
0
5
10
15
20
25
30
t (s)

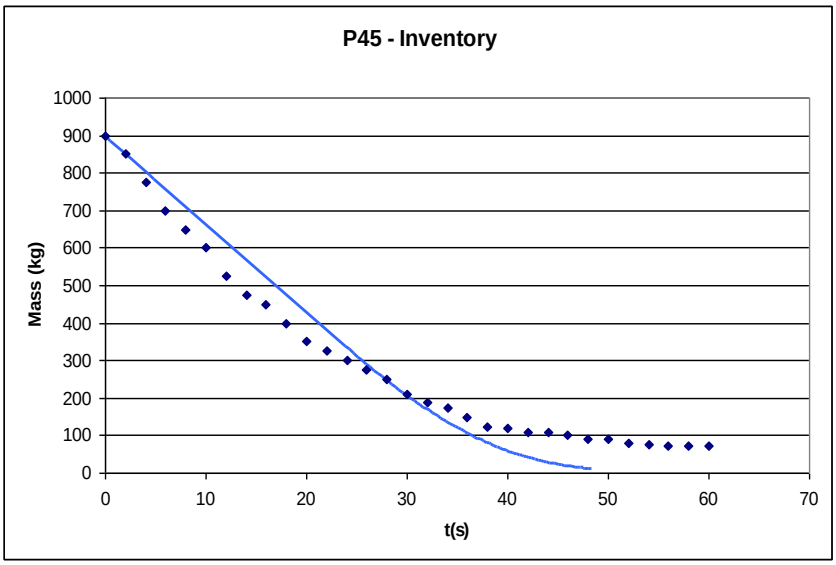
P45 - Inventory
Mass (kg)
1000
900
800
700
600
500
400
300
200
100
0
0
10
20
30
40
50
60
70
t(s)

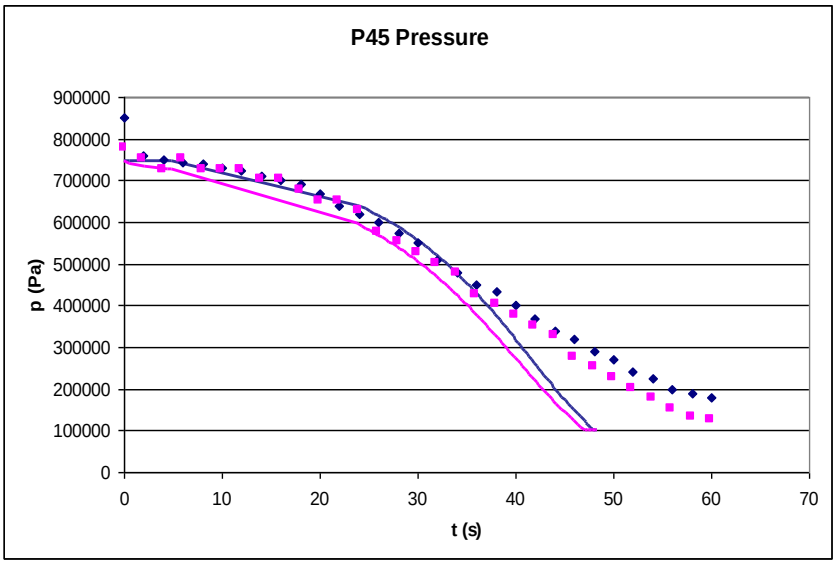
P45 Pressure
p (Pa)
900000
800000
700000
600000
500000
400000
300000
200000
100000
0
0
10
20
30
40
50
60
70
t (s)

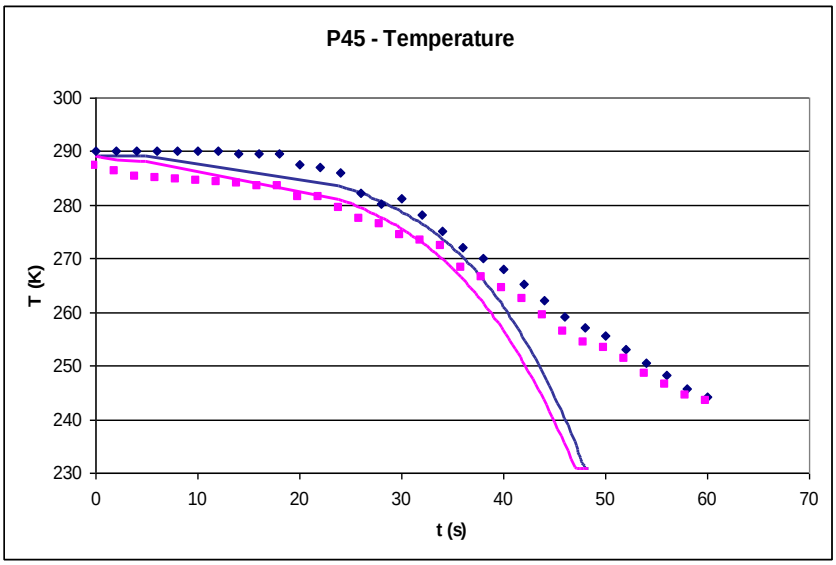
P45 - Temperature
300
290
280
270
260
250
240
230
T (K)
0
10
20
30
40
50
60
70
t (s)


P47 - Inventory
Mass(kg)
1000
900
800
700
600
500
400
300
200
100
0
0
20
40
60
80
100
120
140
160
t(s)

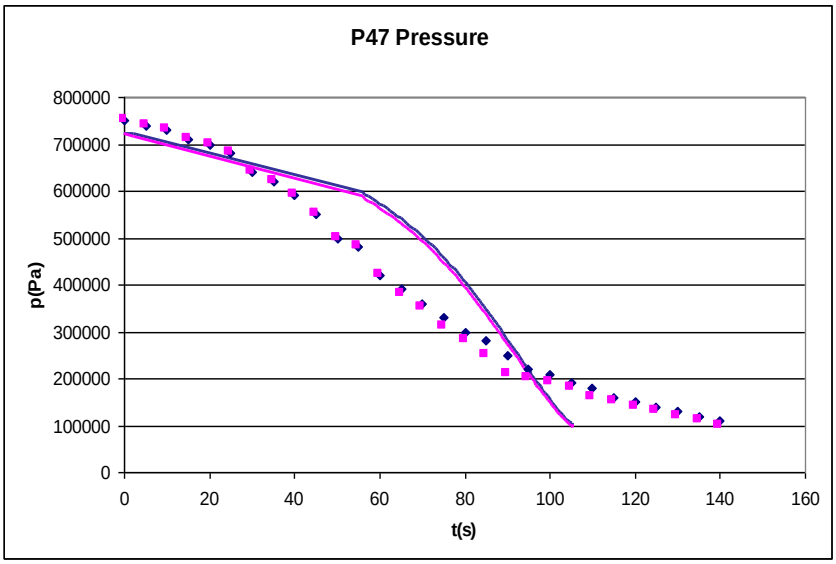
P47 Pressure
p(Pa)
800000
700000
600000
500000
400000
300000
200000
100000
0
0
20
40
60
80
100
120
140
160
t(s)

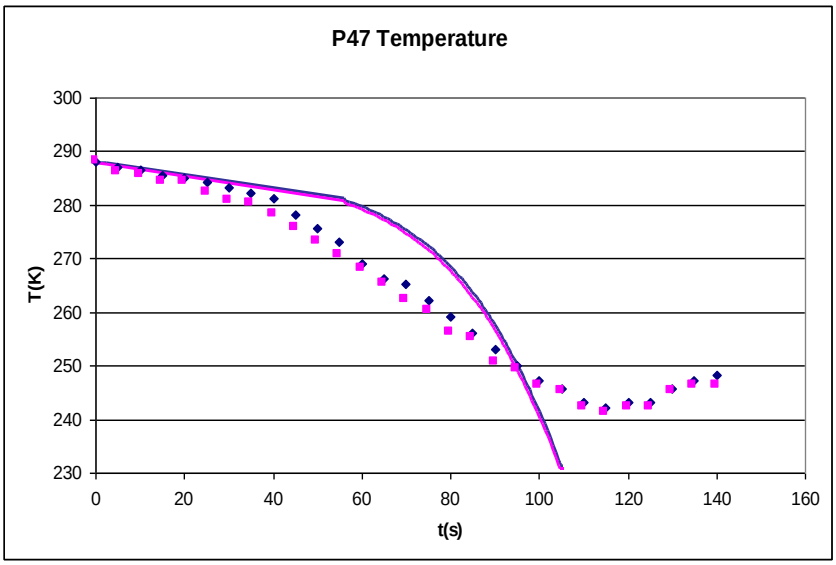
P47 Temperature
300
290
280
270
260
250
240
230
T(K)
0
20
40
60
80
100
120
140
160
t(s)

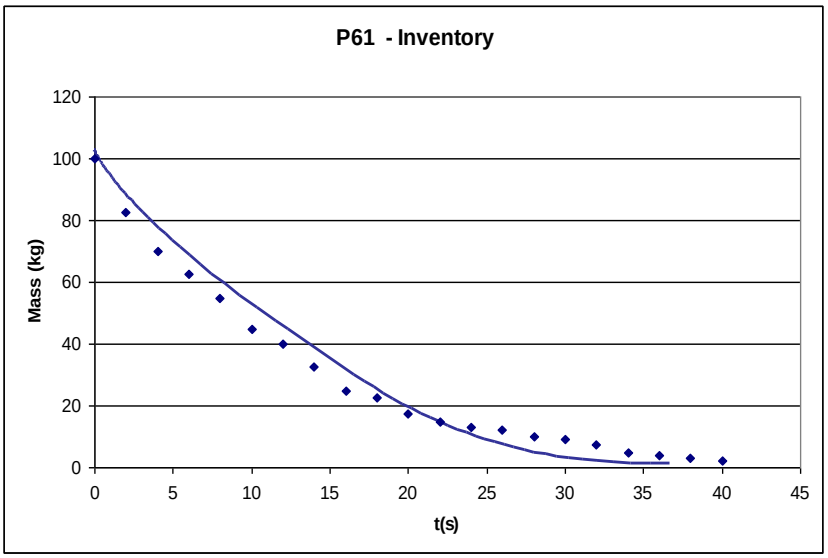
P61 - Inventory
Mass (kg)
120
100
80
60
40
20
0
0
5
10
15
20
25
30
35
40
45
t(s)

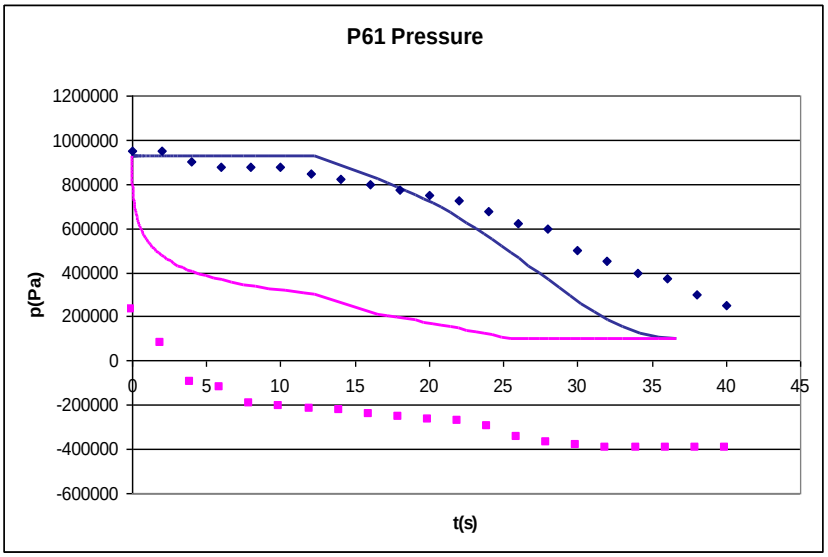
P61 Pressure
p(Pa)
1200000
1000000
800000
600000
400000
200000
0
-200000
-400000
-600000
0
5
10
15
20
25
30
35
40
45
t(s)

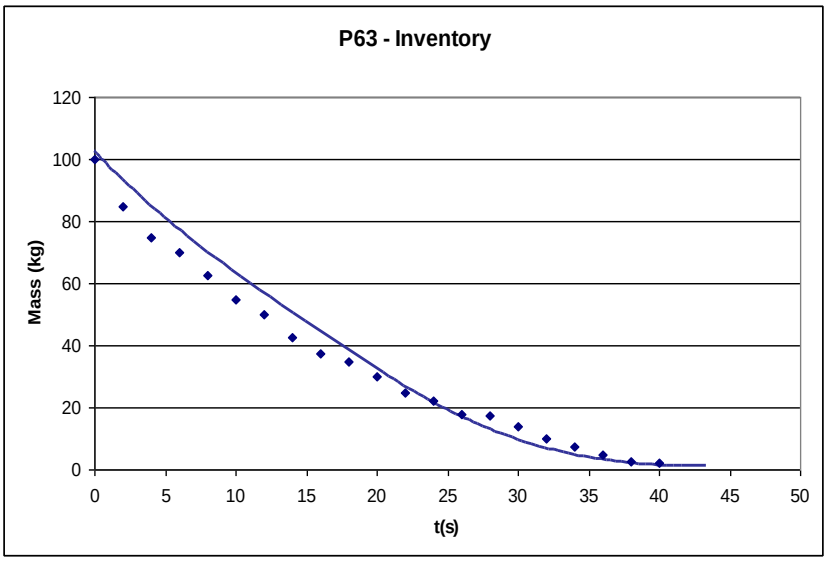
P63 - Inventory
Mass (kg)
120
100
80
60
40
20
0
0
5
10
15
20
25
30
35
40
45
50
t(s)

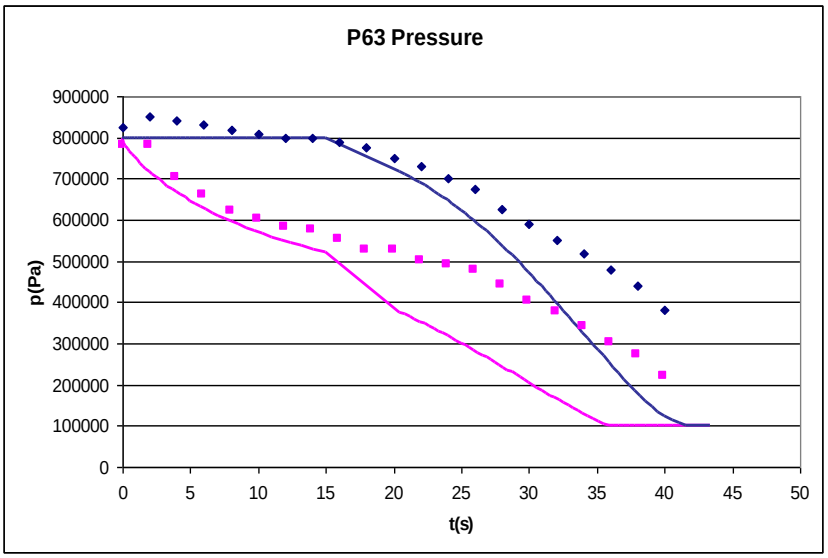
P63 Pressure
p(Pa)
900000
800000
700000
600000
500000
400000
300000
200000
100000
0
0
5
10
15
20
25
30
35
40
45
50
t(s)

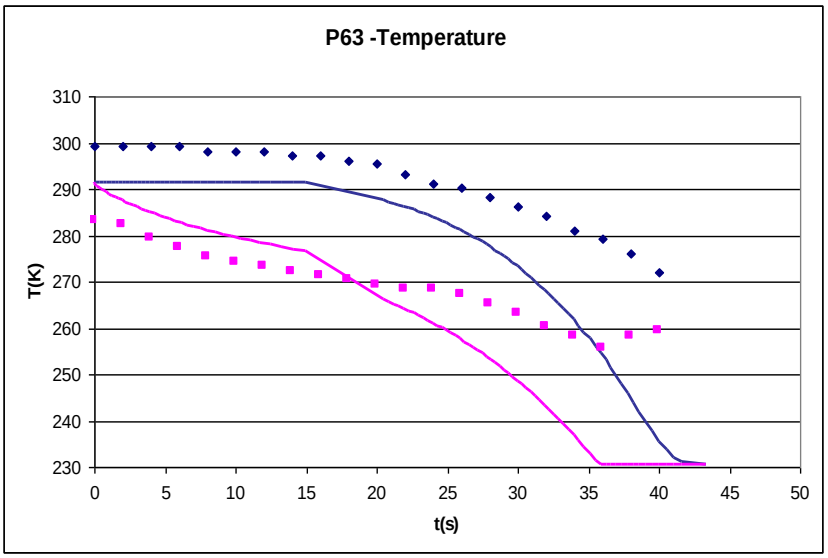
P63 -Temperature
T(K)
310
300
290
280
270
260
250
240
230
0
5
10
15
20
25
30
35
40
45
50
t(s)

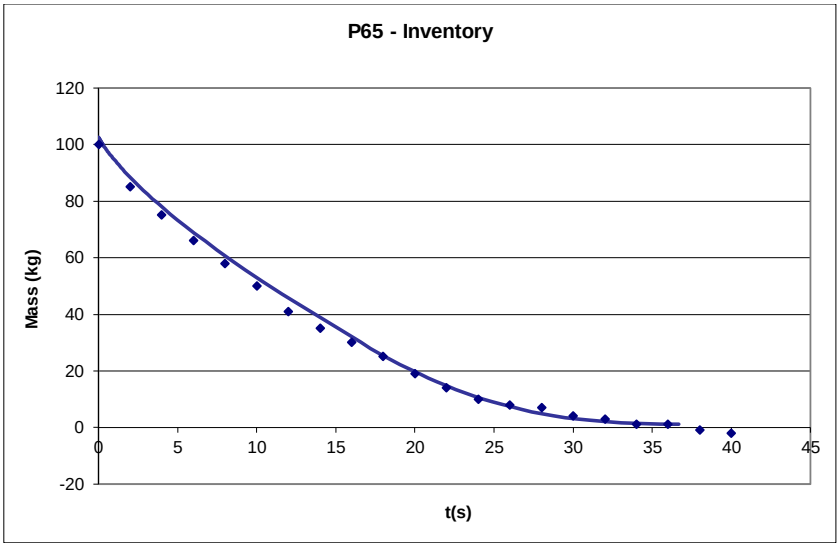
P65 - Inventory
Mass (kg)
120
100
80
60
40
20
0
-20
0
5
10
15
20
25
30
35
40
45
t(s)

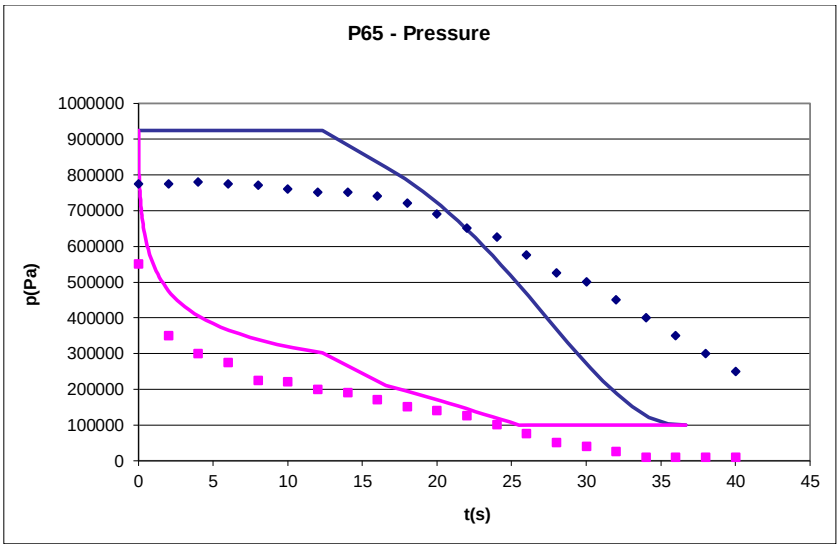
P65 - Pressure
p(Pa)
1000000
900000
800000
700000
600000
500000
400000
300000
200000
100000
0
0
5
10
15
20
25
30
35
40
45
t(s)

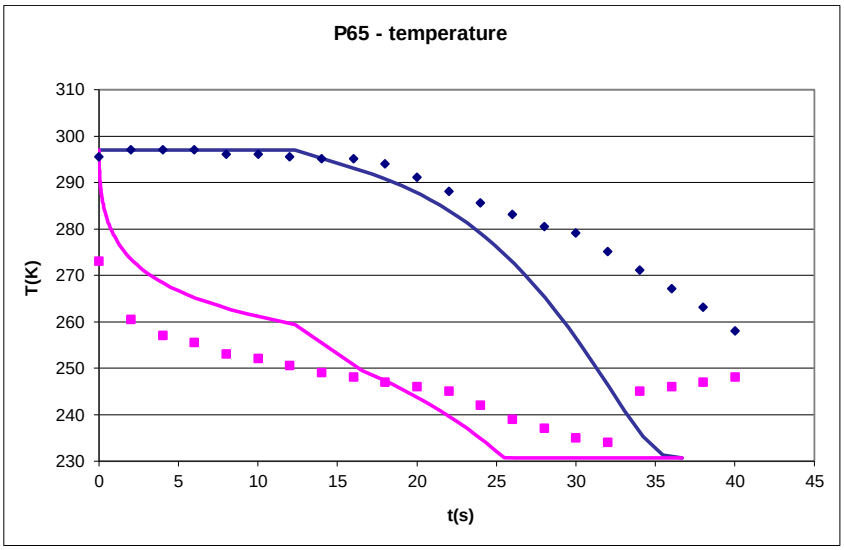
P65 - temperature
T(K)
310
300
290
280
270
260
250
240
230
0
5
10
15
20
25
30
35
40
45
t(s)

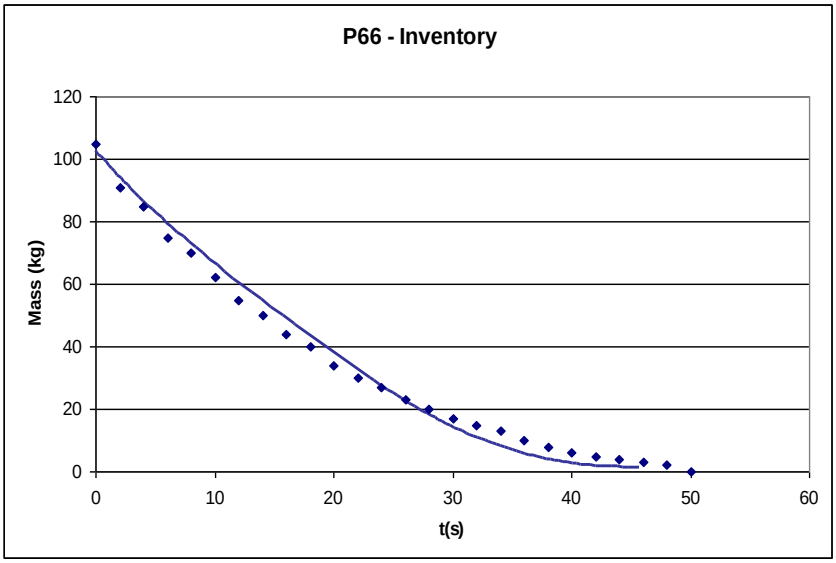
P66 - Inventory
Mass (kg)
120
100
80
60
40
20
0
0
10
20
30
40
50
60
t(s)

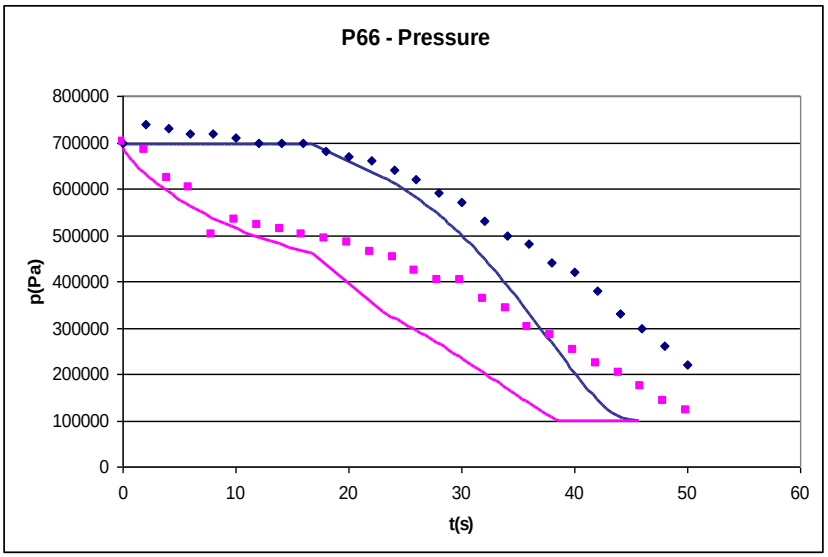
P66 - Pressure
p(Pa)
800000
700000
600000
500000
400000
300000
200000
100000
0
0
10
20
30
40
50
60
t(s)

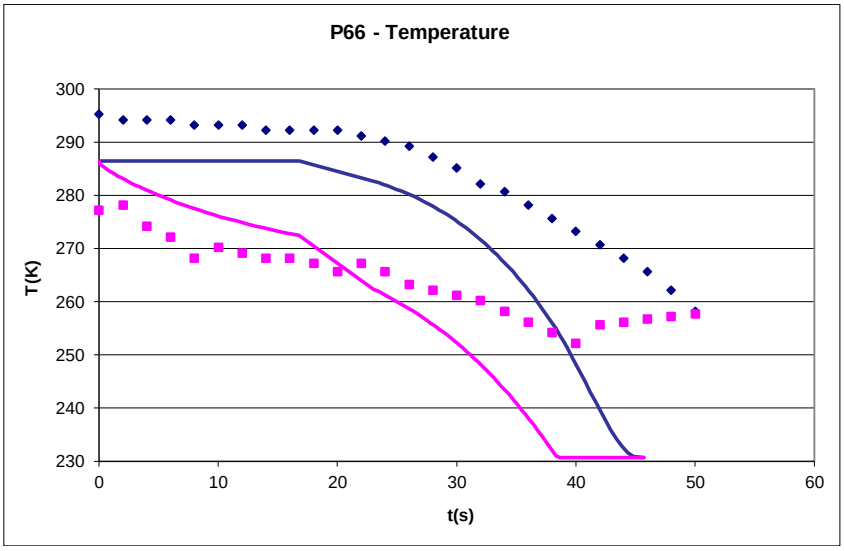
P66 - Temperature
T(K)
300
290
280
270
260
250
240
230
0
10
20
30
40
50
60
t(s)

6 SENSITIVITY ANALYSIS

In addition to the validation described in the previous chapter, a detailed sensitivity analysis has been carried out to analyse the results and to ensure the correctness of the program.

Figure 17 below includes details of the selected basecase values and the parameter variations. The input data that have been varied include all input variables. See Appendix B on further guidance on input and output data for the PIPEBREAK model.

The following basecases have been adopted:

- Basecase A - 100 meter propane pipe, similar to Isle of Grain experiments: limited parameter variations carried out only.
- Basecase B - 35 km propylene pipe: detailed parameter variations carried out as indicated in Figure
- Basecase C - 10 km long ethylene pipe: limited variations carried out only

	D	E	F	L	M	N	O	P	Q
2	**Inputs**		**DNV LONG-PIPELINE MODEL PIPEBREAK**						
3	**Input**	**Description**	**Units**	**Limits**		**basecase A**	**basecase C**	**basecase B**	**Single parameter variation (applied for basecase B)**
4	**Index**			**Lower**	**Upper**				
10	**Fuel properties**								
11	3	material CAS number	-			74986	74851	115071	
12	N	material name	-			PROPANE	ETHYLENE	PROPYLENE	PROPANE, AMMONIA, ETHYLENE, PROPYLENE with amb.temp. = 278.5K
13	**Ambient data**								
14	A	temperature	K	250	325	293.15	253.15	293.15	250, 273.15, 293.15, 313.15, 325K
15	A	pressure	N m-2	50000	120000	100000	100000	100000	0.5, 0.9, 1, 1.1, 1.2 bar
16	A	humidity	-	0	1	0.7	0.7	0.7	0.05,0.5,0.7,0.95
17	**Accident data (top = upstream end of pipe)**								
18	A	total pipe length	m	10	1.00E+05	100	10000	35000	10, 100, 1000, 10000, 35000, 100000m
19	A	pumped in-flow	kg/s	0	1.00E+05	0		0	0, 0.1, 10, 100, 135 (=above maximum) kg/s
20	A	distance of breach from top	m	1	1.00E+05	100	10000	35000	1, 350, 8750, 17500, 26750, 35000m
21	A	relative aperture of breach	fraction	0.5	1	1	1	1	0.8, 0.6, 0.4, 0.2
22	A	breach model (0=correlated, 1=disjoint)	-	0	1.00E+00	1	1	1	0, 1 with full bore rupture at 17500m
23	A	valves close (0=no,1=yes)	-			0	0	0	0, 1 - one valve (vary location/closing time)
24	**Pipe cross-section**								
25	A	pipe inner diameter	m	0.01	2	0.154	0.154	0.154	0.01, 0.04, 0.154, 0.6, 2m
26	A	pipe wall thickness	m	1.00E-04	1	0.0073	0.0073	0.0073	1E-4, 0.073, 0.01, 0.1, 1m
27	A	pipe wall density	kg/m3	1	1.00E+05	7805	7805	7805	1, 10, 100, 1000, 7805, 1E5 kg/m^3
28	A	pipe wall specific heat	J/K/kg	100	1.00E+05	473	473	473	100, 473, 2500, 1E4, 1E5
29	A	pipe roughness	m	1.00E-08	1.00E-03	5.00E-05	5.00E-05	5.00E-05	1E-8, 1E-6, 5E-5, 1E-3m
30	**Valve data**								
31	4	number of valves (don't change)	-	4	4	4	4	4	vary runs with multiple valves
32	5	valve distance from top	m						
33	A	_distance valve 1	m	0	1.00E+05	0	0	0	vary distances before/after flash front etc at time = 1350s after breach
34	A	_distance valve 2	m	0	1.00E+05	0	0	0	
35	A	_distance valve 3	m	0	1.00E+05	0	0	0	
36	A	_distance valve 4	m	0	1.00E+05	0	0	0	
37	6	valve distance from top	s						
38	A	_closure time valve 1	s	0	1.00E+05	1.00E+05	1.00E+05	1.00E+05	vary times before/after flash front etc. at location x=30000m
39	A	_closure time valve 2	s	0	1.00E+05	1.00E+05	1.00E+05	1.00E+05	
40	A	_closure time valve 3	s	0	1.00E+05	1.00E+05	1.00E+05	1.00E+05	
41	A	_closure time valve 4	s	0	1.00E+05	1.00E+05	1.00E+05	1.00E+05	
42	**PARAMETERS (values to be changed by expert users only)**								
43	**Heat transfer**								
44	A	Pipe-fluid thermal coupling	-	0	1	1	1	1	0,1
45	**Numerical control**								
46	7	Suggested nr. of timesteps	-	2	1000	100	100	100	100, 200 varied for valve closing time = 20000s
47	8	Maximum number of data points	-	2	10000	200	150	200	
48	**Ambient Data**								
49	A	molecular weight	kg/kmole	10	100	28.966		28.966	
50	**ATEX model parameters**								
51	A	expansion method (0 - min.therm.change, 1-isentropic, 2-conservation of energy		0	2	2		2	2,1,0
52	A	critical Weber number		1	50	12.5		12.5	
53	A	maximum velocity	m/s	0.01	600	500		500	
54	A	minimum droplet diameter	m	1.00E-08	0.01	1.00E-08		1.00E-08	
55	A	maximum droplet diameter	m	1.00E-08	1	1.00E-02		1.00E-02	

Figure 17. Sensitivity analysis: basecase data and parameter variations

7. REMAINING ISSUES AND FUTURE DEVELOPMENTS

1. Breach

   1.1. Validity of results for smaller breach sizes

   The PIPEBREAK model is expected to result in more accurate predictions for larger aperture fractions, and is expected to be less accurate for aperture fractions of less than 20%. As a result, the minimum allowable value of 20% is currently chosen.

   1.2. Validity of results for length of pipe branch

   The PIPEBREAK model will only be valid if the pipe branch is sufficiently long. This means fL/D is sufficiently large, where f is the Fanning friction coefficient, L the pipe-branch length, and D the inner pipe diameter. In practice this means that ideally fL/D >> 300. For very small pipe-branch lengths PIPEBREAK may have numerical problems and the run may be terminated prematurely.

   1.3. Model selection

   As indicated above, the PIPEBREAK model is not valid for smaller breach sizes and/or short pipes. For these scenarios the existing initial-rate (steady-state) or short-pipe PHAST models should be adopted. Future model-selection logic should be developed to decide between the appropriate model. Also improved modelling for intermediate hole sizes and/or intermediate pipelength's (for which both the PHAST model and PIPEBREAK are not valid) may be developed.

2. Material

   The PIPEBREAK model is currently applicable for pure compounds only. Modelling for multi-compound mixtures may need to involve modelling of multiple flash fronts (corresponding to each individual compound) and is part of potential further work.

   Where pipelines conveying multi-compound mixtures of sub-cooled/flashing liquid are specified in PHAST, these are modelled (i.e., as a 'first-order' approximation) as time-varying leaks from spherical vessels with successful detection and isolation assumed. The 'equivalent' spherical vessel inventory is estimated from pipeline inventory at steady-state storage conditions, while the leak is assumed to conservatively occur at the base of the vessel. For release scenarios involving pumped inflow, an amount of inventory is added to the estimated equivalent spherical vessel inventory. The added inventory corresponds to the normal process pumping throughput multiplied by time to earliest termination of pump inflow by any inline isolation valve. The above approach is likely to provide conservative (higher throughput with shorter times to complete depressurization) source term estimates.

3. Pumps

   3.1. Currently the pump is defined by prescribing a constant flow rate (kg/s) at the upstream pipe end. In future a more advanced pump formulation could be formulated, which would allow the prescription of a 'pump curve' (flow rate as function of pump pressure) instead of a prescribed constant pump flow rate.

   3.2. For low pump flow rates, the flow rate may be insufficient to arrest the flash front and this may cause the pump to fail. This scenario cannot be rigorously modelled by PIPEBREAK, and in such instances, a warning is issued as soon as the flash front hits the pump. Thereafter, the pump is assumed to trip (shutdown) with subsequent outflow based on zero pumped inflow (see regime iii, section 2.5).

4. Valves

   4.1. Numerical problems or inaccurate results

   In case the valve closure cannot be resolved very well by PIPEBREAK, the user is advised to increase the number of timesteps. Note also that PIPEBREAK may decide to close the valve at a slightly earlier timestep, if this time is 'close' to the specified valve closure time. Again this will be modelled more accurately by increasing the number of timesteps.

5. Atmospheric expansion

   5.1. Droplet size diameter

For some cases, the user may need to increase the number of timesteps to ensure a sufficient good resolution for the atmospheric-expansion results output for both branches.

6. Combination of branch contributions

   6.1. Currently it is assumed that both branches point in the same direction, which is a simplified assumption since branches may point in different directions. Also it is currently assumed that the medium surrounding the pipe will not affect the release rate, i.e. effects of crater formation etc. are ignored.

7. Further verification of PIPEBREAK program. This may involve comparison with other, more CPU-intensive software programs, which are based on a more exact solution of the 1D pipe flow equations. This would e.g. test the validity of the parabolic pressure fit.

APPENDICES

Appendix A. A breach along the pipe, with two branches interacting

A.1 The model for two branches interacting at the outflow

Introduction

We shall use the notation established in the previous working papers with subscripts A and B to refer to the two branches - see figures. Consider for the moment a full bore rupture (of total area 2A) in a pipe such that the flows from the two branches interact.

Just behind the orifice we shall define "exit" quantities G and v from the sum of total mass flux density from the two branches defined to be:

$$2G = G_A + G_B \qquad or \qquad 2AG = AG_A + AG_B \tag{62}$$

and the sum of the momentum flux densities defined to be:

$$2G^2 v = G_A^2 v_A + G_B^2 v_B \tag{63}$$

Note that both branches have the same internal area A and so the total mass and momentum fluxes through the orifice are $2GA$ and $2G^2vA$ respectively. In the symmetric case $G=G_A=G_B$ and $v=v_A=v_B$. In general GA is the mean of the two mass fluxes and v is a weighted mean specific volume.

If we think of the streamlines coming together with no compression just behind the orifice we can consider a fictitious flow of mass flux density G and momentum flux density G^2v through a total area 2A.

The choke pressure

If we go back to the case of independent full bore ruptures in Branches A and B then, while they are both choked, there are two independent choke pressures $p_{choke}(A)$ and $p_{choke}(B)$ given by the choke conditions

$$G_A^2 \frac{dv_A}{dp} = -1 \qquad G_B^2 \frac{dv_B}{dp} = -1 \tag{64}$$

For flows which interact at the breach there is only one exit pressure and, with the above idea in mind of simply collecting the streamlines from the two branches, combined with the notion of quasi-steady flow in both Branches A and B, we model the combined choke pressure $p_{choke}(G_A,G_B)$ by

$$\frac{1}{2}\left(G_A^2 \frac{dv_A}{dp} + G_B^2 \frac{dv_B}{dp} \right) = -1 \tag{65}$$

The choke pressure will in general depend on the geometry of the breach, but this would seem to be the simplest possible model, in that in the symmetric case it gives exactly the same choke pressure as in the case of independent branches.

Of course this is a choke pressure appropriate for a mass flux density G coming through an area 2A. For an orifice of reduced total area $2A_x$ ($=2\alpha A$) and mass flux density G_x given by

$$2G_x A_x = 2GA \tag{66}$$

we shall model the choke pressure as

$$p_{choke}(G_A A/A_x, G_B A/A_x) \qquad or \qquad p_{choke}(G_A/\alpha,\ G_B/\alpha) \tag{67}$$

Again in the symmetric case this reduces to the same choke pressure as is defined in the single branch model with an orifice of area $A_x = \alpha A$.

Symmetry and asymmetry

Initially both branches will be considered to hold stationery, saturated liquid. Each will commence in regime ii (described earlier) where the two phase region near the outflow end of the branch eats its way along the branch, eroding the saturated liquid zone. In this regime the rate of outflow and choke pressure are related purely to the length of the two phase zone, and the two branches will behave in a symmetric way, as long as there is no inflow in either branch. However at some stage the flash front will reach the end of the shorter branch and after that the contributions of the two branches will in general differ. (If there is an inflow in one of the two branches, this too will disturb the symmetry.)

Summary

In effect we have defined two new variables G and v and two new equations relating them to the flow variables in each branch. In the case of non-interacting flows, the behaviour of the two branches is unchanged. In the interacting case, we model them as seeing the same choke pressure, as defined above.

A.2 The initial flux from two branches interacting at the outflow

The initial outflow rate is again found by demanding that the choke pressure is the saturated vapour pressure at the initial temperature and as corresponds to pure saturated liquid. This is defined entirely by conditions at the outlet and not by anything to do with the length of the pipe. Therefore G, G_A and G_B will all be initially the same as G was in the single branch problem. With a total aperture of 2A the total outflow rate will be the same (per branch) as it was in the single branch problem.

A.3 The computational algorithm for evolving the flow

The computational algorithm for a single branch

For a single branch A (say) the steps in evolving the flow were very broadly:

1. Choose a new value of G_A
2. Evaluate the exit pressure $p_e(G_A)$ as the maximum of the choke pressure and ambient
3. With this pressure evaluate the state of the fluid and then the time t_A at which G_A is achieved in Branch A

This gives the new value of out flux and the time at which it is achieves and all the thermodynamic properties at the ends of the pipe along the way.

The computational algorithm for two disjoint branches

The procedure for the case of two independent branches will be to evolve each individually and then interpolate the output from each to the same time, before adding the two contributions.

The computational algorithm for interacting branches

At the same level of detail the steps for evolving the interacting flow in the two-branch problem (regarding Branch A as the "primary" branch) are:

1. Choose a new value of G_A

2. With G_A constant at this value, define a function $F(G_B)$ as follows
   (a) evaluate the exit pressure $p_e(G_A, G_B)$ as the maximum of the choke pressure and ambient
   (b) with this pressure evaluate the time t_A at which G_A is achieved in Branch A
   (c) with the same pressure evaluate the time t_B at which G_B is achieved in Branch B
   (d) $F = t_B - t_A$

3. Solve $F(G_B)=0$ for G_B

We now have the evolved values of G_A and G_B and the time taken to evolve to that point. Steps 2(b) and 2(c) are in fact essentially the complete algorithm for a single branch and so this will be rather slower.

In fact the procedure will require that the longer branch or the branch with an inflow is taken to be the primary branch.

Output quantities

For a configuration where two branches are involved, the various output quantities of interest, summed or averaged, as appropriate, over the two branches of the pipe are:

1. Total mass of fluid per unit cross-sectional area in the pipe:

$$M = M_A + M_B$$

2. Total mass of fluid in the pipe:

$$m = AM = AM_A + AM_B$$

3. Mass expelled:

$$m_{\exp elled} = m_{initial} - m + m_{in}$$

where m_{in} is the amount which has flowed in at the upstream end of branch A sinc the initial time t=0 when the pipe contained mass $m_{initial}$.

4. Mass flux:

$$2G_x A_x = 2GA$$

If the two branches are in the interactive configuration, then they see the same pressure at the exit and have the same exit temperature $T=T_A=T_B$ and various other quantities are straightforwardly found:

5. Specific volume:

$$v = \frac{(G_A^2 v_A + G_B^2 v_B)}{2G^2}$$

6. Velocity

$$w = Gv = \frac{(G_A^2 v_A + G_B^2 v_B)}{2G} = \frac{(G_A w_A + G_B w_B)}{2G}$$

7. Quality (liquid mass fracation)

$$y = \frac{(G_A y_A + G_B y_B)}{2G}$$

8. Specific enthalpy

$$h = \frac{(G_A h_A + G_B h_B)}{2G}$$

If the two branches are behaving independently but the outflows mix immediately outside the pipe then there can in principle be heat transfer between the two two-phase streams. However for no interactions to be taking place, the mixing must of necessity occur after the jets have depressurised to ambient pressure - a process which (for choked) flows decreases temperature significantly, and for which one might make jet-model dependent predictions.

Therefore, in the case of disjoint outflows the specific volume, velocity, etc may be regarded only as appropriately weighted averages of the two branches. Nevertheless they may be considered useful, even though they may not be directly measurable.

A.4 Conclusion

This completes the specification of the model for the interacting two-branch (and independent two-branch) case in terms of the equivalent model for a single branch.

The computational procedure for interacting branches is likely to be significantly more CPU-time consuming than for the case of individual or disjoint branches, for which it is optimised. This was part of the reason for introducing the disjoint branch option. And indeed early indications are that the same situation modelled as disjoint or interacting gives very similar results, even in the case where the breach is 20-30% along the length of the pipe, where the difference is potentially largest. (For a breach at either end, both models reduce to the single branch model; for a breach at the mid-point, in a case of zero inflow, the situation is symmetric and the disjoint model will give the same behaviour of the two branches and in particular the exit pressure will be the same, obviating the need for the interacting model to constrain it.)

The disjoint case is therefore considered the default model; the interacting case is there in the first instance for comparison in order to assess whether there is likely to be a difference.

Appendix B. Guidance on input and output data for PIPEBREAK model

B.1 Input data

A list of the input data for the PIPEBREAK model is given by Figure 18. These data are split into the following categories:

1. Input data (always to be specified by the users):

   1.1. Output file. The model produces an output file <filename>.LDT where the specified filename must contain maximum eight characters. Use filename DNW (**D**o **N**ot **W**rite) to suppress writing of an output file. The output files contain certain time-varying discharge data needed for subsequent model linking (dispersion calculations).

   1.2. Fuel properties. The user specifies the material name and the CAS number for the pressurised liquid contained in the pipe. Note that the initial pressure of the liquid in the entire modelled pipe is presumed to be larger than the saturated vapour pressure.

   1.3. Ambient data. The user should specify the ambient data corresponding to the exterior of the pipe:

      1.3.1. temperature T_a (K). This affects only droplet size, as material temperature is specified directly.
      1.3.2. pressure p_a (Pa). Following initial choked flow, unchoked flow occurs at the breach with exit pressure equal to the ambient pressure p_a.
      1.3.3. humidity r_h (fraction). This parameter is only used in the ATEX atmospheric-expansion calculations applied in the case of choked flow. It has only a very slight effect on these calculations.
      1.3.4. Wind speed at release height (m/s). This parameter is only used by the Melhem droplet correlation.

   1.4. Accident data:

      1.4.1. total pipe length L_T (s). This is the total length of the modelled pipe. The distance along the pipe is indicated by x, with the upstream end corresponding to x=0 and the downstream end to x=L_T.
      1.4.2. material temperature T_s (K). PIPEBREAK takes into account the heat transfer from the pipe walls (assumed to be at the initial material temperature T_s) to the pipe fluid.
      1.4.3. pumped in-flow (kg/s). This is the pumped in-flow at the upstream end of the pipe, which is currently assumed to remain constant following the breach.
      1.4.4. distance between breach and upstream end of pipe, x_B (m). This determines the location of the breach. The value of x_B should satisfy $x_B \leq L_T$. Note that in case of $x_B=L_T$ the breach will be at the downstream end of the pipe, and the upstream branch A needs to be modelled only.
      1.4.5. relative aperture of breach , α (fraction). This is the ratio of the area A_{breach} of the breach at the end of the pipe branch and the inner pipe cross-sectional area A, i.e. $\alpha = A_{breach}/A$ with $0.5<\alpha\leq 1$. Note that too small values for α are not allowed, since the PIPEBREAK model is not appropriate for small orifice (pin-hole) areas. Note that α=1 corresponds to a full-bore rupture. The following two cases are considered:
         - breach at the end of the pipe. Only one pipe branch needs to be modelled
         - breach not at the end of the pipe. The pipe is split into two branches with identical breach areas A_{breach} = min(A, A_{hole}/2) = α A, where A_{hole} is total leak area. The post-expansion discharge results for each branch are combined to obtain the total discharge data. Herewith it is assumed that both branches point in the same direction, and 'coalesce' to an effective orifice of area 2 A_{breach}.
      1.4.6. breach model: 0 = correlated (interactive) or 1 = disjoint. The user should at present always adopt the disjoint model. The correlated model is at present not robust.
      1.4.7. parameter specifying whether valve close: i_{valve} = 0 (no) or i_{valve} = 1 (yes). In case valve are closing, the user need to specify the valve data (see below)

   1.5. Pipe cross-section data:
      1.5.1. pipe inner diameter D (m). The circular inner cross-section of the pipe is assumed to be uniform along the entire pipe.
      1.5.2. pipe wall thickness Y (m)
      1.5.3. pipe wall density (kg/m^3)
      1.5.4. pipe wall specific heat (J/kg/K)
      1.5.5. pipe roughness z_o (m). Fanneløp recommends taking a roughness length for the inner pipe wall z_0=1.3 10^{-5}m (0.0005 inches) in the absence of any better information. See also Section 2.6.1.

   1.6. Valve data. In case the user indicates that valves close (see above; i_{valve} = 1), he needs to specify the following data:
      1.6.1. Total number of valves present along the modelled pipe, n_{valve}
      1.6.2. For each valve i = 1,…n_{valve}:
         - distance x_i (m) of valve from upstream end of pipe
         - the type of valve:
            - 0 (closure at specified closure time)
            - 1 (closure when flow rate exceeds specified flow rate)
            - 2 (non-return valve, i.e. closure when flow reverses direction).
         - valve d,ata depending on type of valve:
            - 0 – nd valve closure time t_i (s) from start of breach.
            - 1 - excess flow rate (kg/s)
            - 2 - not/applicable (no data needed)
      1.6.3. For all types of valves, the valve is assumed to close instantaneously. Thus following a valve closure, the pipe length is effectively reduced, with a new closed pipe-end boundary condition adopted at the valve location Excess flow

valves may close for both branches, while non-return valves will only have an effect for the downstream branch B.

2. Parameters (input data to the changed by expert users only)

2.1. Heat transfer

2.1.1. Pipe-fluid thermal coupling
- 0 – ignore heat transfer effects from the pipe wall to the fluid
- 1 – model transfer from the pipe wall to the fluid

2.2. Numerical control

2.2.1. suggested number of time steps, n_{time}. This is the approximate number of time steps, for which results are output by PIPEBREAK. The recommended number is 100 time steps, but in case of presence of valves, the user may need to increase this. Note that increase of this number, will increase the accuracy but increase the CPU time. In case of any numerical problems (or weird looking results e.g. in case of valves), the user is recommended to increase n_{time}.

2.2.2. maximum number of time steps, n_{max}. This is the maximum number of time steps, which will be output. This should be considerable larger than the above suggested number of time steps, n_{time}. The recommended number is n_{max} = 200 time steps.

2.2.3. maximum release duration (s). The discharge calculations are terminated after the maximum release duration is reached, or earlier in cases where the pipe is completely depressurized before maximum release duration is reached. Default value 3600 s.

2.3. Ambient data: molecular weight (kg/kmole)

2.4. Atmospheric-expansion (ATEX) model parameters. These parameters only affect the atmospheric-expansion calculations in case of choked flow. See the ATEX theory manual for further details. The parameters are as follows:

2.4.1. type of method of expansion calculations
2.4.2. critical Weber number (-)
2.4.3. flag for final velocity cap: 0 (user input) or 1 (sonic speed)
2.4.4. maximum velocity (m/s); only used in case above flag equals 0
2.4.5. minimum droplet diameter (m)
2.4.6. maximum droplet diameter (m)
2.4.7. correlation for SMD (Sauter Mean Diameter) droplet size. Available correlations:
2.4.7.1. 0 – the original CCPS (Phast 6.4) method – default in Phast 6.6 and earlier versions.
2.4.7.2. 1 – the JIP method uses the correlation proposed by the Flashing Liquid Jets Phase II project.
2.4.7.3. 2 – the TNO Yellow Book correlation
2.4.7.4. 3 – the droplet size correlation developed by Tilton and Farley
2.4.7.5. 4 – the Melhem correlation.
2.4.7.6. 5 – the correlation proposed in the JIP Phase III
2.4.7.7. 6 – the Modified CCPS correlation – new default in Phast 6.7
2.4.7.8. 7 – the Modified CCPS correlation but not for two-phase pipes

Of these only the Original CCPS, Modified CCPS, Melhem and JIP phase III correlations are available in Phast, with the Modified CCPS correlation as the default.

2.4.8. do not force droplet-size correlation (0), force use of droplet-size correlation applicable for mechanical break-up (1) or force use of droplet-size correlation applicable for flashing break-up (2)

	A	B	C	D	E	F	L	M	N	O	P
10				3	Output file (DNW=Do Not Write file)	-			DNW		
11	**Fuel properties**										
12				4	material CAS number	-			74986	74986	74986
13				N	material name	-			propane		
14	**Ambient data**										
15				A	temperature	K	200	350	293.15		
16				A	pressure	N m-2	50000	120000	100000		
17				A	humidity	-	0	1	0.7		
18				A	Wind speed at release height	m/s	0	100	5		
19	**Accident data (top = upstream end of pipe)**										
20				A	total pipe length	m	10	1.00E+06	100		
21				A	Material temperature	K	200	3.50E+02	293.15		
22				A	pumped in-flow	kg/s	0	1.00E+05	0		
23				A	distance of breach from top	m	1	1.00E+06	100	50	
24				A	relative aperture of breach	fraction	0.2	1	1		0.5
25				A	breach model (0=correlated, 1=disjoint)	-	0	1	1		
26				A	valves close (0=no,1=yes)	-	0	1	0		
27	**Pipe cross-section**										
28				A	pipe inner diameter	m	0.01	2	0.154		
29				A	pipe wall thickness	m	1.00E-04	1	0.0073		
30				A	pipe wall density	kg/m3	1	1.00E+05	7805		
31				A	pipe wall specific heat	J/K/kg	100	1.00E+05	473		
32				A	pipe roughness	m	1.00E-08	1.00E-03	5.00E-05		
33	**Valve data**										
34				5	number of valves (don't change)	-	4	4	4		
35				6	valve distance from top	m					
36				A	_distance valve 1	m	0	1.00E+06	0		
37				A	_distance valve 2	m	0	1.00E+06	0		
38				A	_distance valve 3	m	0	1.00E+06	0		
39				A	_distance valve 4	m	0	1.00E+06	0		
40				7	valve type array (0 -closure time, 1- excess flow,2 - non-return)						
41				A	_type valve 1	-	0	2	0		
42				A	_type valve 2	-	0	2	0		
43				A	_type valve 3	-	0	2	0		
44				A	_type valve 4	-	0	2	0		
45				8	valve data array (type 0 - closure time from start, type1 - excessflowrate)						
46				A	_closure time or exc. flow rate valve 1	s or kg/s	0	1.00E+05	1.00E+05		
47				A		s or kg/s	0	1.00E+05	1.00E+05		
48				A	_closure time or exc. flow rate valve 3	s or kg/s	0	1.00E+05	1.00E+05		
49				A	_closure time or exc. flow rate valve 4	s or kg/s	0	1.00E+05	1.00E+05		
50	**PARAMETERS (values to be changed by expert users only)**										
51	**Heat transfer**										
52				A	Pipe-fluid thermal coupling (0 = off, 1= model pipe-fluid heat transfer)	-	0	1	0		
53	**Numerical control**										
54				8	Suggested nr. of timesteps	-	2	1000	100		
55				9	Maximum number of data points	-	2	10000	200		
56				A	maximum release duration	s	0	1.00E+08	3600		
57	**Ambient Data**										
58				A	molecular weight	kg/kmole	10	100	28.966		
59	**ATEX model parameters**										
60				A	expansion method (0 - min.therm.change, 1-isentropic, 2-conservation of energy		0	2	2		
61				A	critical Weber number		1	50	12.5		
62				A	Maximum velocity capping flag (0 - user, 1 - sonic)	-	0	1	0		
63				A	maximum velocity	m/s	0.01	1000	500		
64				A	minimum droplet diameter	m	0.00E+00	0.01	1.00E-08		
65				A	maximum droplet diameter	m	0.00E+00	1	1.00E-02		
66				A	Droplet correlation (0=original CCPS, 1= JIPII,2=TNO,3=Tilton,4=Melhem,5=JIPIII, 6 = modified CCPS, 7= modified CCPS excl. 2PH pipe)	-	0	7	6		
67				A	Force mechanical or flashing breakup (0=No, 1=force mech., 2=force flashing)	m	0	2	0		

Figure 18. Input data for PIPEBREAK model

The above input data are derived from the generic spreadsheet for PIPEBREAK. For each input parameter a brief description of the meaning of the parameter is given, its unit, and its lower and upper limits. Column N contains a complete list of input data corresponding to the example for a full-bore rupture at the end of the pipe. Columns O, P, Q indicate those values that need to be changed to invoke (O) a full-bore rupture in the pipe middle, (P) a 50% partial breach at the pipe and (Q) a 50% partial breach in the pipe middle.

B.2 Model run and output data

PIPEBREAK calculations are carried out as described in the computational procedure (see Sections 2.10 and A.3). The output data are listed by
Figure 19. These output data are split into the following categories:

1. Fanning coefficient (see Section 2.6.1)

2. Data for output branch A (upstream to breach; $0 < x < x_B$)

    2.1. Time for end of choked flow (s). This is the duration of the initial phase of choked flow after the start of the breach occurrence.
    2.2. Time for flash front to hit the pipe end (s). This is the end time for regime ii (see Figure 1).
    2.3. Time for branch depressurised (s). This is the time at which the exit flow reduces to zero. It is the end time for regime iii (see Figure 3).
    2.4. Number of timesteps output for branch A
    2.5. For each timestep the following data:
        2.5.1. time t_A since start of breach (s)
        2.5.2. data at upstream end of branch A (x=0): flow rate (kg/s), temperature (K), pressure (Pa), velocity (m/s), liquid mass fraction (-). Note that the flow rate is directly derived from the pump inflow rate (= 0 kg/s in absence of pump). In case of no pumped-in flow the flow rate and velocity will be zero.
        2.5.3. orifice data at breach [at downstream end of branch A ($x = x_B$)] prior to atmospheric expansion (flashing): flow rate (kg/s), temperature (K), pressure (Pa), velocity (m/s), liquid mass fraction (-).
        2.5.4. pipe masses:
            2.5.4.1. active mass (kg),which can potentially be released from branch A. This equals the pipe total mass in the pipe if no valves are present or have yet been closed for branch A. In other cases, it equals the total mass, minus the mass which has been trapped by closed valves.
            2.5.4.2. pipe total mass (kg), including mass possibly trapped by closed valves
            2.5.4.3. pipe expelled mass (kg). This is the total mass which has been expelled since the start of the breach.
        2.5.5. two-phase length (m). This is the length of the two-phase zone, which increases from 0 m at the onset of the breach (time t = 0) to the entire length of branch A (unless valve close).
        2.5.6. post-flash data at breach [at downstream end of branch A ($x = x_B$)] after atmospheric expansion: (m/s), liquid mass fraction (-) and droplet diameter (m). Note that the post-expansion pressure equals the ambient pressure P_a, and the post-expansion temperature the saturated temperature at P_a. After the end of choked flow, the post-expansion data will be equal to the pre-expansion data.

3. Data for output branch B (downstream to breach; $x_B < x < L_T$). Note that this branch will not be present if the breach is at the end of the pipe ($x_B = L_T$).

    3.1. Time for end of choked flow (s). This is the duration of the initial phase of choked flow after the start of the breach occurrence.
    3.2. Time for flash front to hit the pipe end (s). This is the end time for regime ii (see Figure 1).
    3.3. Time for branch depressurised (s). This is the time at which the exit flow reduces to zero. It is the end time for regime iii (see Figure 3).
    3.4. Number of timesteps output for branch B
    3.5. For each timestep the following data:
        3.5.1. time t_B since start of breach (s)
        3.5.2. data at upstream end of branch B ($x=L_T$): flow rate (kg/s), temperature (K), pressure (Pa), velocity (m/s), liquid mass fraction (-). Note that the flow rate is directly derived from the pump inflow rate (= 0 kg/s in absence of pump). In case of no pumped-in flow the flow rate and velocity will be zero.
        3.5.3. orifice data at breach [at downstream end of branch B ($x = x_B$)] prior to atmospheric expansion (flashing): flow rate (kg/s), temperature (K), pressure (Pa), velocity (m/s), liquid mass fraction (-).
        3.5.4. pipe masses:
            3.5.4.1. active mass (kg),which can potentially be released from branch B. This equals the pipe total mass in the pipe if no valves are present or have yet been closed for branch B. In other cases, it equals the total mass, minus the mass which has been trapped by closed valves.
            3.5.4.2. pipe total mass (kg), including mass possibly trapped by closed valves.
            3.5.4.3. pipe expelled mass (kg). This is the total mass which has been expelled since the start of the breach.
        3.5.5. two-phase length (m). This is the length of the two-phase zone, which increases from 0 m at the onset of the breach (time t = 0) to the entire length of branch B (unless valve close).
        3.5.6. post-flash data at breach [at downstream end of branch B ($x = x_B$)] after atmospheric expansion: (m/s), liquid mass fraction (-) and droplet diameter (m). Note that the post-expansion pressure equals the ambient pressure P_a, and the post-expansion temperature the saturated temperature at P_a. After the end of choked flow, the post-expansion data will be equal to the pre-expansion data.

4. Data for total pipe ($0 < x < L_T$; sum of contributions for branch A, $0 < x < x_B$) and branch B ($x_B<x<L_T$). The number of timesteps output equals precisely the suggested number of timesteps specified as input. For each timestep the following data are produced:

    4.1. Number of timesteps output for combined contributions
    4.2. time t_T since start of breach (s)
    4.3. averaged specific volume (m^3/kg). This is a mass-weight average of the specific volumes for branches A and B.
    4.4. averaged post-flash velocity (m/s). This is a mass-weighted average of the post-flash velocities for branches A and B
    4.5. averaged post-flash liquid mass fraction (-). This is a mass-weighted average of the post-flash liquid mass fractions for branches A and B
    4.6. averaged post-flash droplet diameter (m/s). This is a mass-weighted average of the post-flash droplet diameters for branches A and B

4.7. pipe active mass (kg), excluding mass potentially trapped by closed valves. It is the sum of the pipe active masses for branches A and B.
4.8. pipe total mass (kg), including mass possibly trapped by closed valves. It is the sum of the pipe total masses for branches A and B.
4.9. pipe expelled mass (kg). This is the total mass which has been expelled since the start of the breach. It is the sum of the pipe expelled for branches A and B.
4.10. pipe expelled mass rate (kg/s). This is the sum of the mass rates for branches A and B.

	D	E	F	L	M	N	O	P	Q
57	**Outputs**								
58	**Output**	**Description**	**Units**						
59	**Index**								
60		***ERROR STATUS***				***OK***	***OK***	***OK***	***OK***
61	1	Double precision output array	-						
62	A	Fanning coefficient	-			3.80E-03	3.80E-03	3.80E-03	3.80E-03
63	**Output branch A**								
64	A	A - time for end of choked flow	s			1.91E+01	8.35E+00	2.53E+01	1.17E+01
65	A	A - time for flash front to hit end	s			7.71E+00	3.06E+00	7.76E+00	2.57E+00
66	A	A - time for branch depressurised	s			2.35E+01	9.60E+00	2.77E+01	1.23E+01
67	2	A - number of timesteps	-			105	94	69	60
68	3	A - time	s			Array	Array	Array	Array
69	4	A - upstream flow rate	kg/s			Array	Array	Array	Array
70	5	A - upstream temperature	K			Array	Array	Array	Array
71	6	A - upstream pressure	Pa			Array	Array	Array	Array
72	7	A - upstream velocity	m/s			Array	Array	Array	Array
73	8	A - upstream liquid mass fraction	fraction			Array	Array	Array	Array
74	9	A - orifice flow rate	kg/s			Array	Array	Array	Array
75	10	A - orifice temperature	K			Array	Array	Array	Array
76	11	A - orifice pressure	Pa			Array	Array	Array	Array
77	12	A - orifice velocity	m/s			Array	Array	Array	Array
78	13	A - orifice liquid mass fraction	fraction			Array	Array	Array	Array
79	14	A - pipe active mass	kg			Array	Array	Array	Array
80	15	A - pipe total mass	kg			Array	Array	Array	Array
81	16	A - pipe expelled mass	kg			Array	Array	Array	Array
82	17	A - two-phase length	m			Array	Array	Array	Array
83	18	A - post-flash velocity	m/s			Array	Array	Array	Array
84	19	A - post-flash liquid mass fraction	fraction			Array	Array	Array	Array
85	20	A - post-flash droplet size	m			Array	Array	Array	Array
86	**Output branch B**								
87	A	B - time for end of choked flow	s			0.00E+00	8.35E+00	0.00E+00	1.17E+01
88	A	B - time for flash front to hit end	s			1.00E+128	3.06E+00	1.00E+128	2.57E+00
89	A	B - time for branch depressurised	s			1.00E+128	9.60E+00	1.00E+128	1.23E+01
90	21	B - number of timesteps	-			0	94	0	60
91	22	B - time	s			Array	Array	Array	Array
92	23	B - upstream flow rate	kg/s			Array	Array	Array	Array
93	24	B - upstream temperature	K			Array	Array	Array	Array
94	25	B - upstream pressure	Pa			Array	Array	Array	Array
95	26	B - upstream velocity	m/s			Array	Array	Array	Array
96	27	B - upstream liquid mass fraction	fraction			Array	Array	Array	Array
97	28	B - orifice flow rate	kg/s			Array	Array	Array	Array
98	29	B - orifice temperature	K			Array	Array	Array	Array
99	30	B - orifice pressure	Pa			Array	Array	Array	Array
100	31	B - orifice velocity	m/s			Array	Array	Array	Array
101	32	B - orifice liquid mass fraction	fraction			Array	Array	Array	Array
102	33	B - pipe active mass	kg			Array	Array	Array	Array
103	34	B - pipe total mass	kg			Array	Array	Array	Array
104	35	B - pipe expelled mass	kg			Array	Array	Array	Array
105	36	B - two-phase length	m			Array	Array	Array	Array
106	38	B - post-flash velocity	m/s			Array	Array	Array	Array
107	37	B - post-flash liquid mass fraction	fraction			Array	Array	Array	Array
108	39	B - post-flash droplet size	m			Array	Array	Array	Array
109	**Output total pipe (T)**								
110	40	T - number of timesteps	-			105	94	69	60
111	41	T - time	s			Array	Array	Array	Array
112	42	T - average specific volume	m3/kg			Array	Array	Array	Array
113	43	T - average post-flash velocity	m/s			Array	Array	Array	Array
114	44	T - post-flash liquid mass fraction	fraction			Array	Array	Array	Array
115	45	T - average post-flash droplet size	m			Array	Array	Array	Array
116	46	T - pipe active mass	kg			Array	Array	Array	Array
117	47	T - pipe total mass	kg			Array	Array	Array	Array
118	48	T - pipe expelled mass	kg			Array	Array	Array	Array
119	49	T - pipe expelled mass rate	kg/s			Array	Array	Array	Array

Figure 19. **Output data for PIPEBREAK model**

The above output data are derived from the generic spreadsheet for PIPEBREAK. The values of the three runs in columns N,O,P,Q correspond to the input values included in columns N,O,P,Q of Figure 18. Output data for the discharge array data are not included in this figure.

From the output data the following can typically be observed for both upstream and downstream branches in the case of absence of valves and pump:

1. immediate depressurisation to the saturated vapour pressure along the entire pipe
2. flash propagation away from the breach towards the pipe end. Initially choked flow at the breach and subsequent unchoked flow. For a short pipe, the flash front will typical hit the pipe end prior to the onset of unchoked flow, while for a sufficiently long pipe unchoked flow will commence prior to the flash front reaching the pipe end. Until the flash front hits the pipe end, the data at the pipe end will not change and correspond to 100% liquid, with the pressure equal to the saturated vapour pressure $p_v(T_a)$.
3. After the flash front hits the upstream pipe end, depressurisation at the pipe end to the atmospheric pressure P_a.

B.3 Detailed information on PIPEBREAK errors and warnings

Below information on errors/warnings/messages are given, which can currently be produced by the PIPEBREAK model.

Error messages

```
1       "Unspecified error encountered"
2       "The model does not exist"
3       "The output cache is missing"
4       "Output requested out of range of the steps performed"
5       "The substance data have not been constructed"
6       "An illegal output call has been made for the current branch/disjoint option"
7       "An illegal reference has been made to a non-branch of the pipe"
8       "Evolution of the primary branch of the flow has failed to converge"
9       "Evolution of the secondary branch of the flow has failed to converge"
13      "Zero divide"
```

All the above messages are from internal program errors. Please check possibly other additional warnings for possible reasons. Possible reasons of these problems may be e.g. (a) the use of the correlated (interactive) breach model, which is not advised, or (b) too much heat transfer which caused the liquid phase to dry out. Please contact DNV for further assistance if needed.

```
10      "Computation of the initial mass flux has failed - probably owing to being too close to
        the critical point"
11      "Construction of the model has failed - probably owing to ambient temperature being above
        the critical point"
```

The specified ambient temperature must be always below the critical temperature for PIPEBREAK. If the ambient temperature is above the critical point, the fuel is vapour and the use of the pure-vapour model GASPIPE is recommended.

```
12      "You have chosen interactive double branch model with valves closing.  This combination
        is not available"
```

The use of the interactive breach model is not advised. Suggest to use disjoint breach model.

```
14      "The model is limited to pure compounds and cannot be run for mixtures"
```

PIPEBREAK cannot deal with a pipe filled with a multi-compound pressurised liquid, since it does not allow for modelling of several flash fronts (corresponding to each compound) within the pipe. In case of a multi-compound mixture, the user is suggested to approximate the multi-compound mixture as a pure compound of which the saturated vapour pressure etc. represents most the multi-compound mixture.

```
15      "The calculations to perform the expansion to atmospheric pressure has produced a pure
        vapour jet"
```

The current PIPEBREAK implementation assumes that two-phase to two-phase expansion always occurs immediately downstream of the orifice.

```
201     "The inflow is larger than the predicted maximum release rate"
```

This message is produced if the pump inflow rate is larger than the exit flow rate predicted by PIPEBREAK.

349 "The material temperature is below the fluid's boiling point at ambient pressure."

The model cannot handle sub-cooled liquids so the specified material temperature cannot be below the boiling point at ambient pressure.

351 "An excess flow valve would close in normal operation."

This error is issued when an excess flow valve is present with a pumped pipe inflow larger than the closure limit for the valve, i.e. the valve would close under normal operation of the pipe.

352 "Breach location exceeds total pipe length."

This error is issued when the user has specified a breach location that is larger than the total pipe length.

Warning messages

1007 "Valve closure has not been very well resolved: try requesting more steps."
1008 "Valve closure has not been resolved: try requesting more steps."

Above messages are associated with an inaccurate interpolation to the valve closure time, the first one if it doesn't succeed very accurately and the second if it fails completely. For both cases, it probably means that the original timestep was too small and the user should request more time steps.

1013 "Long pipeline criterion f L/D > 3 not satisfied"

This warning is produced when the long pipe scenario is used, while the long pipeline criterion fL/D > rlong is not satisfied (rlong = 3). Here f is the fanning friction coefficient, L the pipe length and D the inner diameter. In case this warning is given, the line rupture scenario (short pipe) may be considered to be applied instead of the long pipeline scenario. This particularly applies if fL/D <1, although for larger values the long pipeline model could still give more accurate results than the short pipe scenario.

Information messages

2003 "The flash front has encountered the pump. Flow rate from branch A subsequently set equal to pumped inflow"

This message will occur in the case of the presence of a pump, when the flash front hits the pump (upstream end). This will occur, when the pumped inflow is insufficient to arrest the flash front, before it hits the pump. The model subsequently terminates the calculation in the upstream branch and sets the flow rate from the branch equal to the pumped inflow. NB! There is a bug (SI10537) whereby any closure valve will never close in the upstream branch after a flash front has hit the pump, resulting in too large discharge mass from this branch.

2005 The liquid phase has dried out taking the model beyond its limits of applicability"

This will typically happen in case of 'large heat transfer', caused by small pipe diameters, small pipe wall thickness, or large pipe specific heat. The user should check if a realistic pipe has been modelled. If this would be the case, he may wish to consider reducing or switching off the pipe-fluid thermal coupling.

2006 "The arrays provided are too small to contain all output data: larger arrays are recommended"

This message occur if PIPEBREAK requires more numerical steps (for either branch A or branch B), than the maximum size of the output arrays. Thus not all results will be output. In this case, the user is advised to increase the maximum size of the output arrays to ensure that all data are output.

2009 "The orifice velocity prior to the expansion to atmospheric pressure is larger than the user supplied maximum velocity"

The ATEX expansion model (conservation of energy assumptions) adopts a maximum cut-off velocity of the post-expansion velocity (input parameter). A warning is given if the orifice velocity prior to the expansion is larger than this cut-off velocity.

2010 "Solid effects in pipe prior to breach are not modelled but may occur in Branch A after %1%Time%"

This message is issued when the orifice pressure of branch A drops below the triple point pressure of the material – e.g. for CO_2 releases when the orifice pressure drops below its triple point pressure 5.2 bar.

2011 "Solid effects in pipe prior to breach are not modelled but may occur in Branch B after %1%Time%"

Equivalent to 1010, but applicable to branch B.

2012 "Solid effects during atmospheric expansion are not modelled but may occur"

This message is issued for materials with triple point pressures above ambient pressure with the important exception of CO¬2 as the atmospheric expansion model does handle solid CO2 effects.

NOMENCLATURE

a	$[EM^{-1}T^{-2}]$	coefficient in $\psi(T)$
A	$[L^2]$	inner pipe cross-sectional area
A	$[ML^{-1}t^{-2}]$	coefficient in the Clausius-Clapeyron vapour pressure correlation
b	$[EM^{-1}T^{-1}]$	coefficient in $\psi(T)$
B	[T]	coefficient in the Clausius-Clapeyron vapour pressure correlation
c	$[EM^{-1}T^{-1}]$	specific heat
c	$[EM^{-1}]$	coefficient in $\psi(T)$
D	[L]	inner pipe diameter.
E	$[EM^{-1}=L^2t^{-2}]$	(specific) stagnation enthalpy
f		Fanning friction coefficient
G	$[ML^{-2}t^{-1}]$	mass flux density
h	$[EM^{-1}=L^2t^{-2}]$	specific enthalpy
k		a profile integral (=1)
L	[L]	pipe length
M	$[ML^{-2}]$	mass of fluid in the pipe per unit cross-sectional area
p	$[ML^{-1}t^{-2}]$	pressure
q	$[EL^{-2}t^{-1}=Mt^{-3}]$	heat flux density from the pipe wall
t	[t]	time
T	[T]	temperature
v	$[L^3M^{-1}]$	specific volume
w	$[Lt^{-1}]$	fluid flow velocity
x	[L]	distance (downstream from the upstream end of the pipe or upstream from the downstream end of the pipe according to convenience).
Y	[L]	pipe wall thickness
z_0	[L]	inner pipe wall roughness length
α		dimensionless fractional aperture
α		coefficient in $v_L(T)$
η		liquid mass fraction (quality)
λ		a profile parameter (=1)
Λ		coefficient in $v_L(T)$
ρ	ML^{-3}	density
ϕ	$[ML^{-1}t^{-2}]$	T dp/dT along the vapour pressure curve

Subscripts:

0	upstream end of the flow
2	pertaining to the two-phase flow zone
a	ambient/atmospheric
c	at critical point
e	downstream (exit) end of the flow
init	Initial conditions (at time t=0)
L	liquid phase
r	"reduced" - eg $T_r = T/T_c$
s	steel pipe
sat	at saturation (on/along the vapour pressure curve)
v	vapour phase
x	within the orifice

The dimensions given in the above table are:

L=length, t=time, M=mass, T=temperature, and for convenience $E \equiv ML^2t^{-2}$=energy.

All of the equations in this paper are dimensionally correct and so quoting actual units here would be superfluous. (Any units, SI, British Imperial, or American, may be used to evaluate the formulae as long as they are applied consistently. Where values are quoted we have done so in SI.)

About DNV

We are the independent expert in risk management and quality assurance. Driven by our purpose, to safeguard life, property and the environment, we empower our customers and their stakeholders with facts and reliable insights so that critical decisions can be made with confidence. As a trusted voice for many of the world's most successful organizations, we use our knowledge to advance safety and performance, set industry benchmarks, and inspire and invent solutions to tackle global transformations.

Digital Solutions

DNV is a world-leading provider of digital solutions and software applications with focus on the energy, maritime and healthcare markets. Our solutions are used worldwide to manage risk and performance for wind turbines, electric grids, pipelines, processing plants, offshore structures, ships, and more. Supported by our domain knowledge and Veracity assurance platform, we enable companies to digitize and manage business critical activities in a sustainable, cost-efficient, safe and secure way.

DNV | digital@dnv.com | dnv.com/digital

REFERENCES

[1]Webber, D.M., Fanneløp, T.K., and Witlox, H.W.M., "Source Terms from Two-Phase Flow in Long Pipelines following an Accidental Breach", in "International Conference and Workshop on Modeling and Mitigating the Consequences of Accidental Releases of Hazardous Materials", AIChE 1999 ISBN 0-8169-0781-1, pp. 145-167 (1999)

[2] Cowley, L.T., and V.H.Y. Tam, V.H.Y., "Consequences of pressurised LPG releases: the Isle of Grain full scale experiments", GASTECH 88, 13th International LNG/LPG Conference, Kuala Lumpur (1988)

[3] Richardson, S.M. and Saville, G., "Blow-down of LPG Pipelines", Trans. I.Chem.E 74B, pp. 235-244 (1996)

[4] Fanneløp, T.K., and Ryhming, I.L., "Massive release of gas from long pipelines", AIAA Journal of Energy 6, pp. 132-140 (1982)

[5] Leung, J.C., "A generalised correlation for one-component homogeneous equilibrium flashing choked flow", AIChE Journal 32**,** pp. 1743-1746 (1986)

[6] Reid, R.C., Prausnitz, J.M. , and Poling, B.C., "The Properties of Liquids and Gases", 4th Edn., McGraw Hill (1987)

[7] Fanneløp, T.K., "Fluid Mechanics for Industrial Safety and Environmental Protection", Elsevier ISBN 0-444-89863-8 (1994)

[8] Atkins, P.W., "Physical Chemistry", 5th Edition, Oxford University Press, Oxford (1994)

[9] Holt, A., Topalis, P., Witlox, H.W.M., and Clements, F., 'Atmospheric expansion model (ATEX)', DNV, London (2001)